Global QCD analysis of transverse momentum dependent and collinear parton distribution functions

Patrick Barry, Jefferson Lab

Parton Distributions and Nucleon Structure, INT, September 15th, 2022

Complicated Inverse Problem

- Factorization theorems involve convolutions of hard perturbatively calculable physics and non-perturbative objects

$$\frac{d\sigma}{d\Omega} \propto \mathcal{H} \otimes f = \int_x^1 \frac{d\xi}{\xi} \mathcal{H}\left(\frac{x}{\xi}\right) f(\xi)$$

- Parametrize the non-perturbative objects and perform global fit

Experiments to probe pion structure

Drell-Yan (DY)

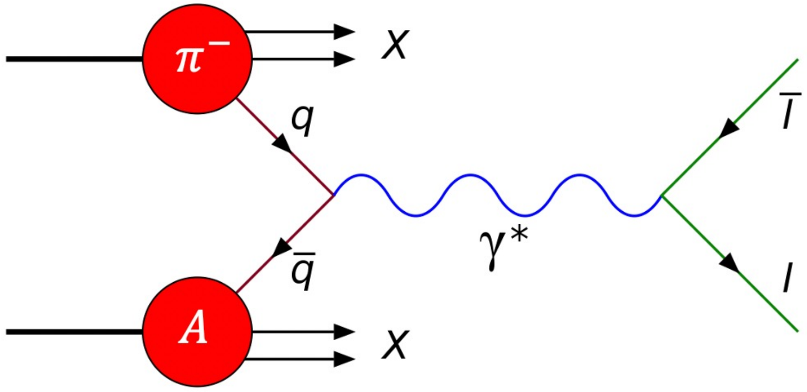

Leading Neutron (LN)

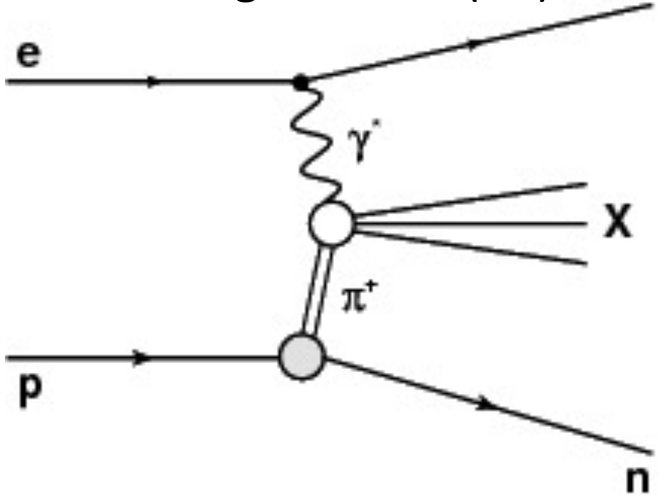

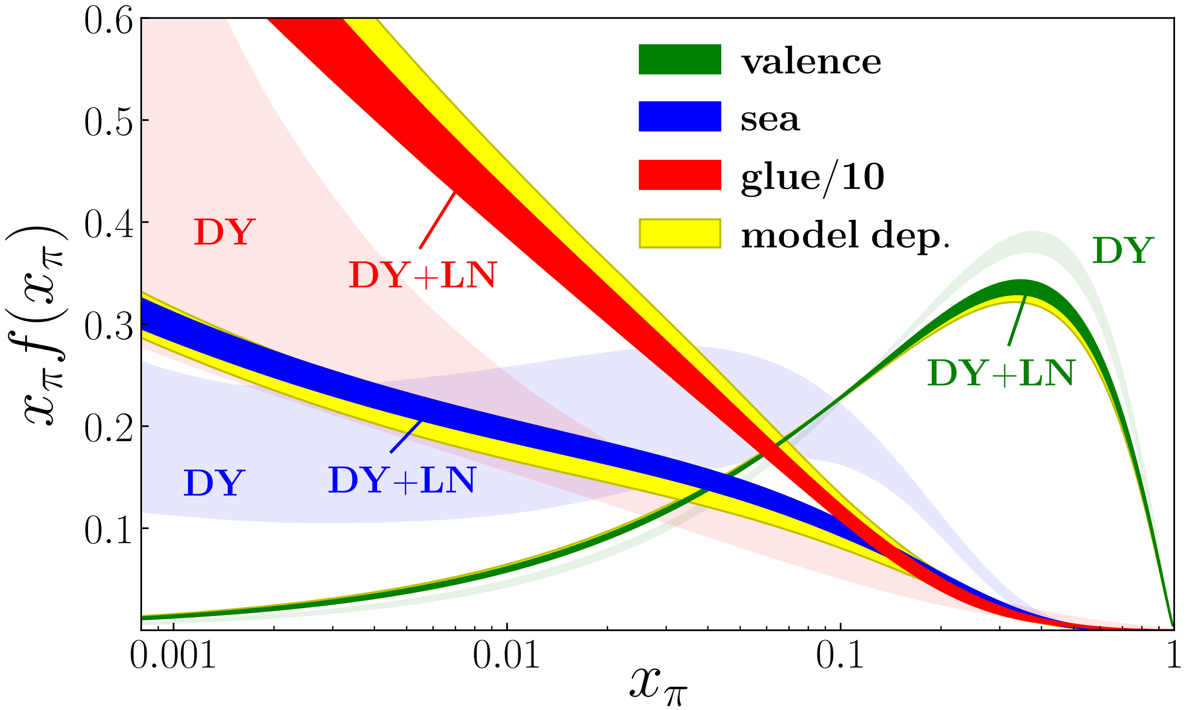

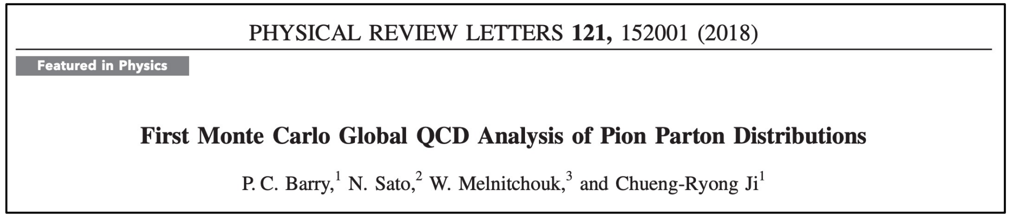

PHYSICAL REVIEW LETTERS **121,** 152001 (2018)

Featured in Physics

First Monte Carlo Global QCD Analysis of Pion Parton Distributions

P. C. Barry,[1] N. Sato,[2] W. Melnitchouk,[3] and Chueng-Ryong Ji[1]

Drell-Yan (DY)

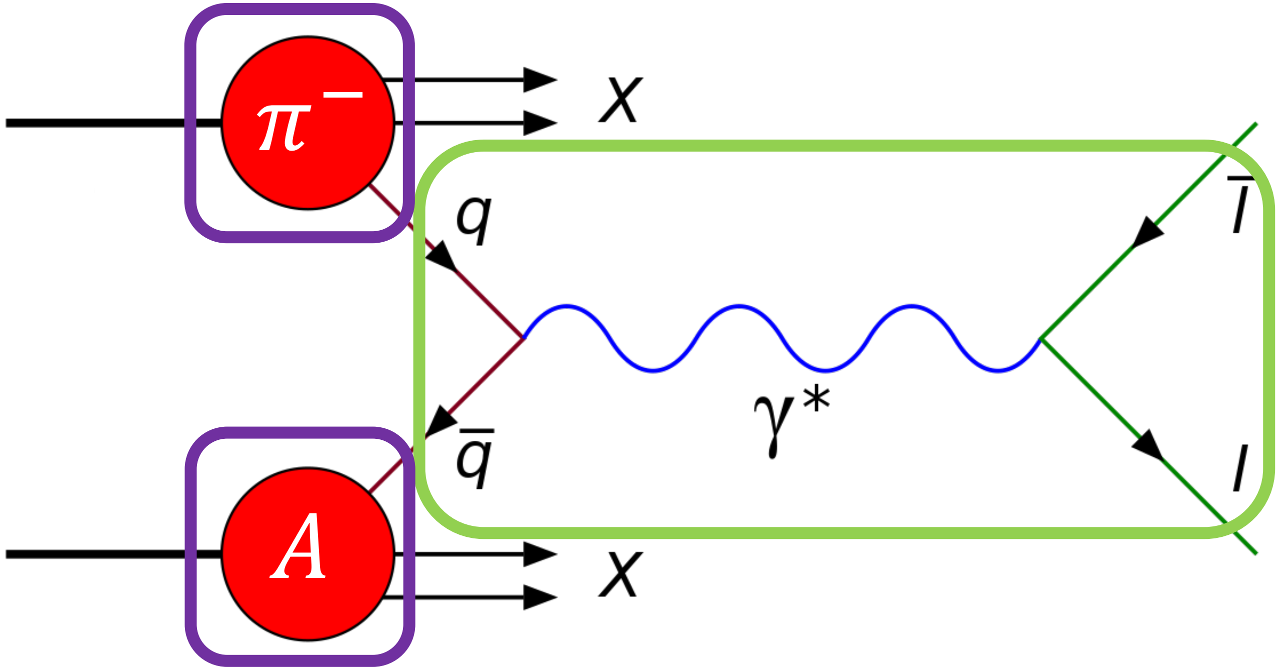

$$\sigma \propto \sum_{i,j} f_i^{\pi}(x_\pi, \mu) \otimes f_j^{A}(x_A, \mu) \otimes C_{i,j}(x_\pi, x_A, Q/\mu)$$

JAM analysis with threshold resummation

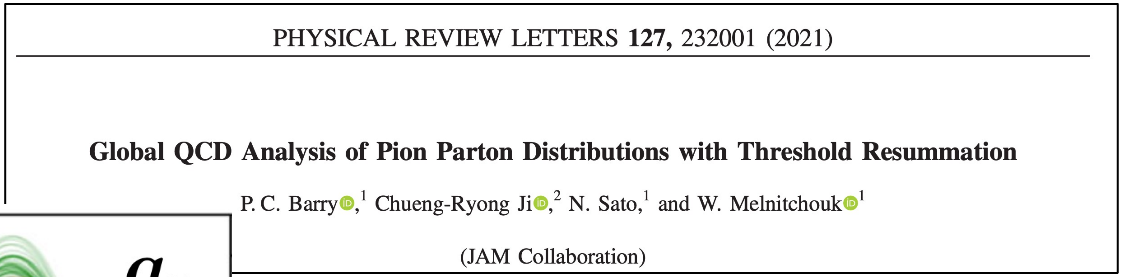
PHYSICAL REVIEW LETTERS **127,** 232001 (2021)

Global QCD Analysis of Pion Parton Distributions with Threshold Resummation

P. C. Barry,[1] Chueng-Ryong Ji,[2] N. Sato,[1] and W. Melnitchouk[1]

(JAM Collaboration)

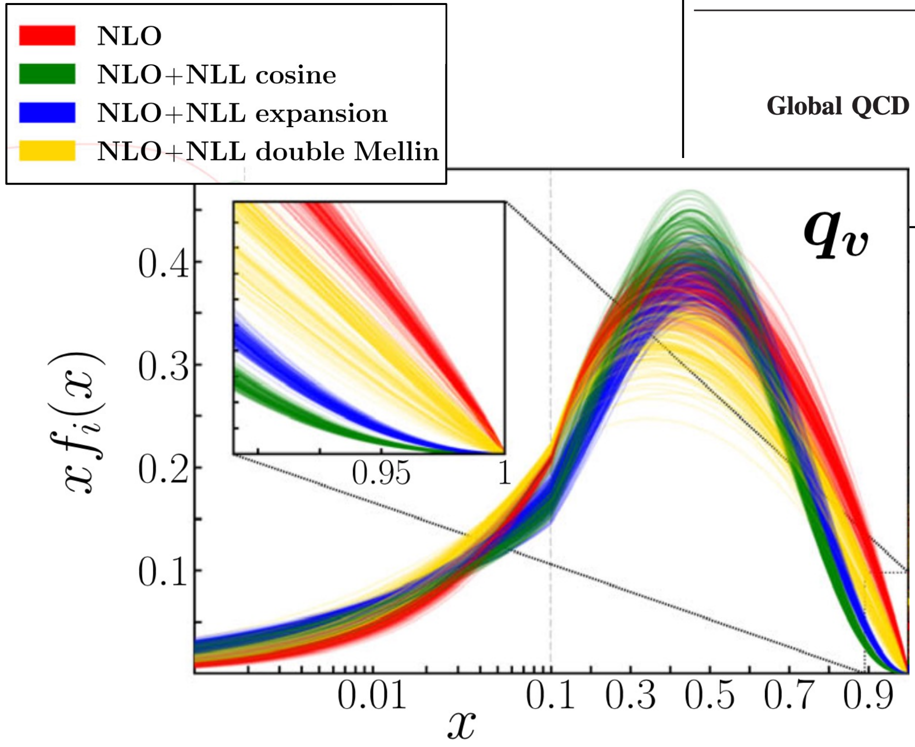

- Highly dependent on perturbative approach
- NLO and NLO+NLL double Mellin methods better on theoretical grounds

$$\beta_{\rm eff}(x,\mu) = \frac{\partial \log |q_v(x,\mu)|}{\partial \log(1-x)}$$

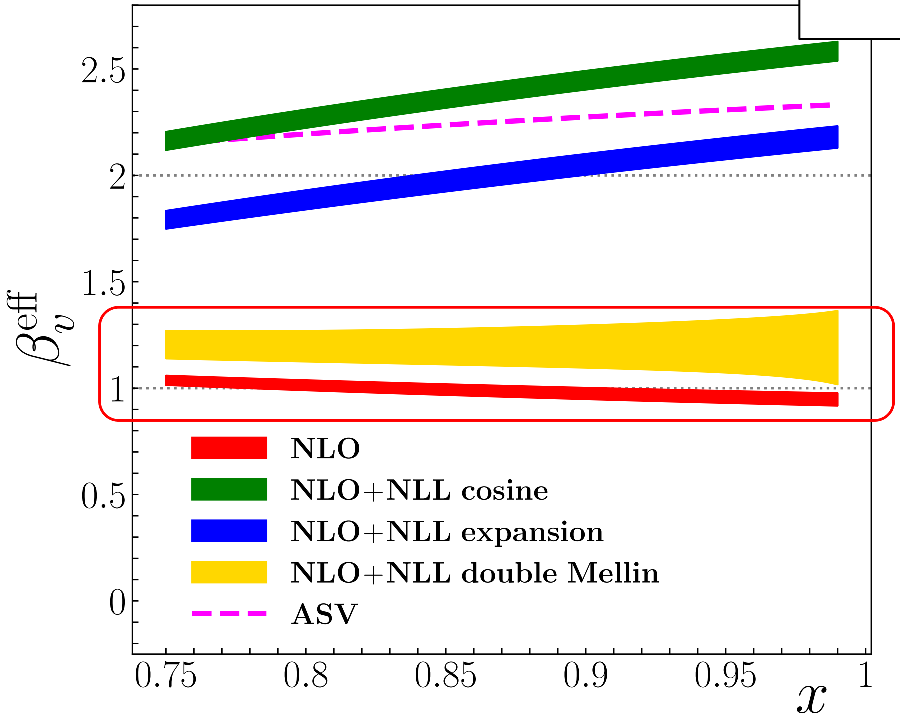

Including lattice QCD data from HadStruc

- Can lattice QCD simulations help to constrain pion distributions?

PHYSICAL REVIEW D **105,** 114051 (2022)

Complementarity of experimental and lattice QCD data on pion parton distributions

P. C. Barry,[1] C. Egerer,[1] J. Karpie,[2] W. Melnitchouk,[1] C. Monahan,[1,3] K. Orginos,[1,3] Jian-Wei Qiu,[1,3] D. Richards,[1] N. Sato,[1] R. S. Sufian,[1,3] and S. Zafeiropoulos[4]

(Jefferson Lab Angular Momentum (JAM) and HadStruc Collaborations)

Goodness of fit

- Scenario A: experimental data alone
- Scenario B: experimental + lattice, no systematics
- Scenario C: experimental + lattice, with systematics

			Scenario A		Scenario B		**Scenario C**	
			NLO	$+\mathrm{NLL_{DY}}$	NLO	$+\mathrm{NLL_{DY}}$	NLO	$+\mathrm{NLL_{DY}}$
Process	Experiment	N_{dat}	$\overline{\chi}^2$		$\overline{\chi}^2$		$\overline{\chi}^2$	
DY	E615	61	0.84	0.82	0.83	0.82	**0.84**	**0.82**
	NA10 (194 GeV)	36	0.53	0.53	0.52	0.54	**0.52**	**0.55**
	NA10 (286 GeV)	20	0.80	0.81	0.78	0.79	**0.78**	**0.87**
LN	H1	58	0.36	0.35	0.39	0.39	**0.37**	**0.37**
	ZEUS	50	1.56	1.48	1.62	1.69	**1.58**	**1.60**
Rp-ITD	a127m413L	18	–	–	1.04	1.06	**1.04**	**1.06**
	a127m413	8	–	–	1.98	2.63	**1.14**	**1.42**
Total		**251**	**0.82**	**0.80**	**0.89**	**0.92**	**0.85**	**0.87**

Effective β from $(1-x)^{\beta_{\text{eff}}}$

$$\beta_{\text{eff}}(x,\mu) = \frac{\partial \log |q_v(x,\mu)|}{\partial \log(1-x)}$$

Calculations from QCD do not predict $\beta_{\text{eff}} = 2$

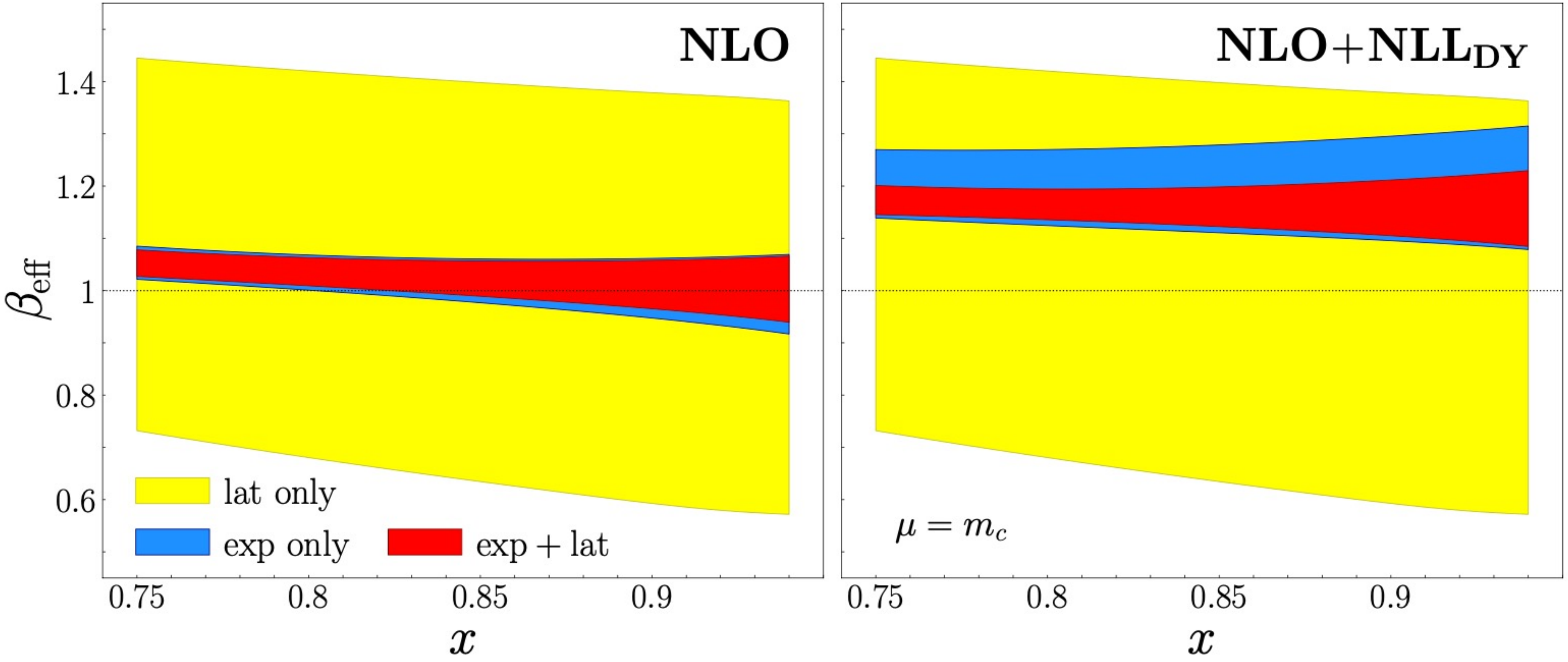

What about the transverse direction?

- The E615 π-induced fixed-target DY experiment measured the transverse momentum spectrum of the $\mu^+\mu^-$
- JAM was able to fit the large-q_T through collinear factorization

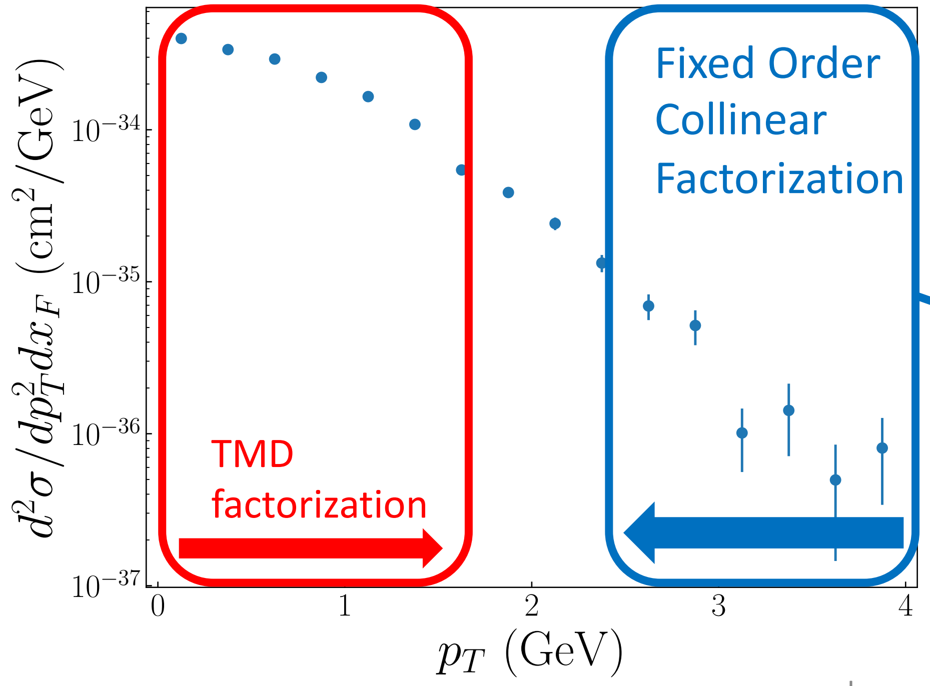

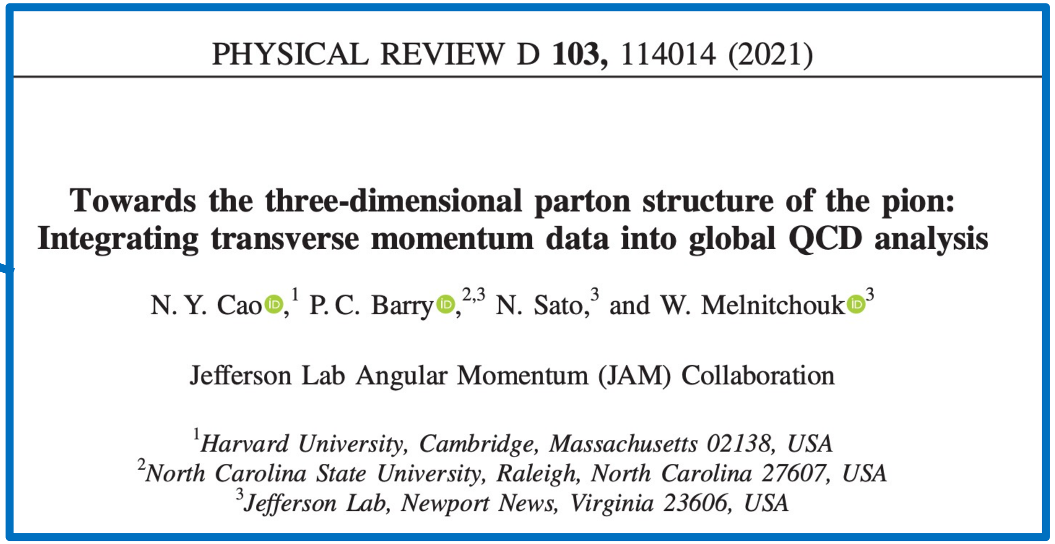
PHYSICAL REVIEW D **103,** 114014 (2021)

Towards the three-dimensional parton structure of the pion: Integrating transverse momentum data into global QCD analysis

N. Y. Cao,[1] P. C. Barry,[2,3] N. Sato,[3] and W. Melnitchouk[3]

Jefferson Lab Angular Momentum (JAM) Collaboration

[1]*Harvard University, Cambridge, Massachusetts 02138, USA*
[2]*North Carolina State University, Raleigh, North Carolina 27607, USA*
[3]*Jefferson Lab, Newport News, Virginia 23606, USA*

Drell-Yan (DY)

- p_T dependent DY in collinear factorization

$$\frac{d\sigma}{dQ^2 dY dp_T^2} = \frac{4\pi\alpha^2}{3N_C Q^2 S} \sum_{i,j} e_q^2 \int_{x_\pi^0}^{1} dx_\pi f_i^\pi(x_\pi, \mu) f_j^A(x_A, \mu) \times \frac{d\hat{\sigma}_{i,j}}{dQ^2 d\hat{t}}$$

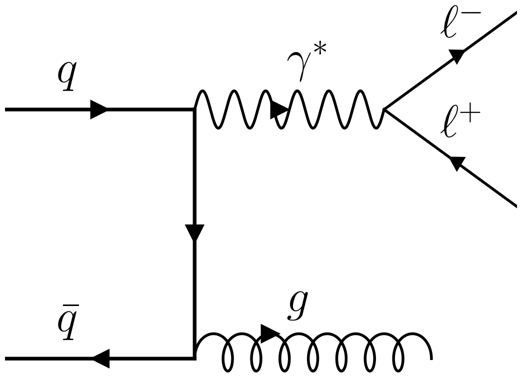

$q\bar{q}$ channel example

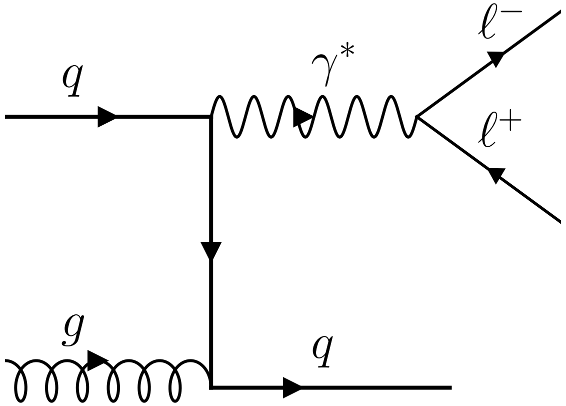

qg channel example

Effects of Each Dataset

- Not much impact from the transverse-momentum dependent DY data
- Data are quite noisy statistically

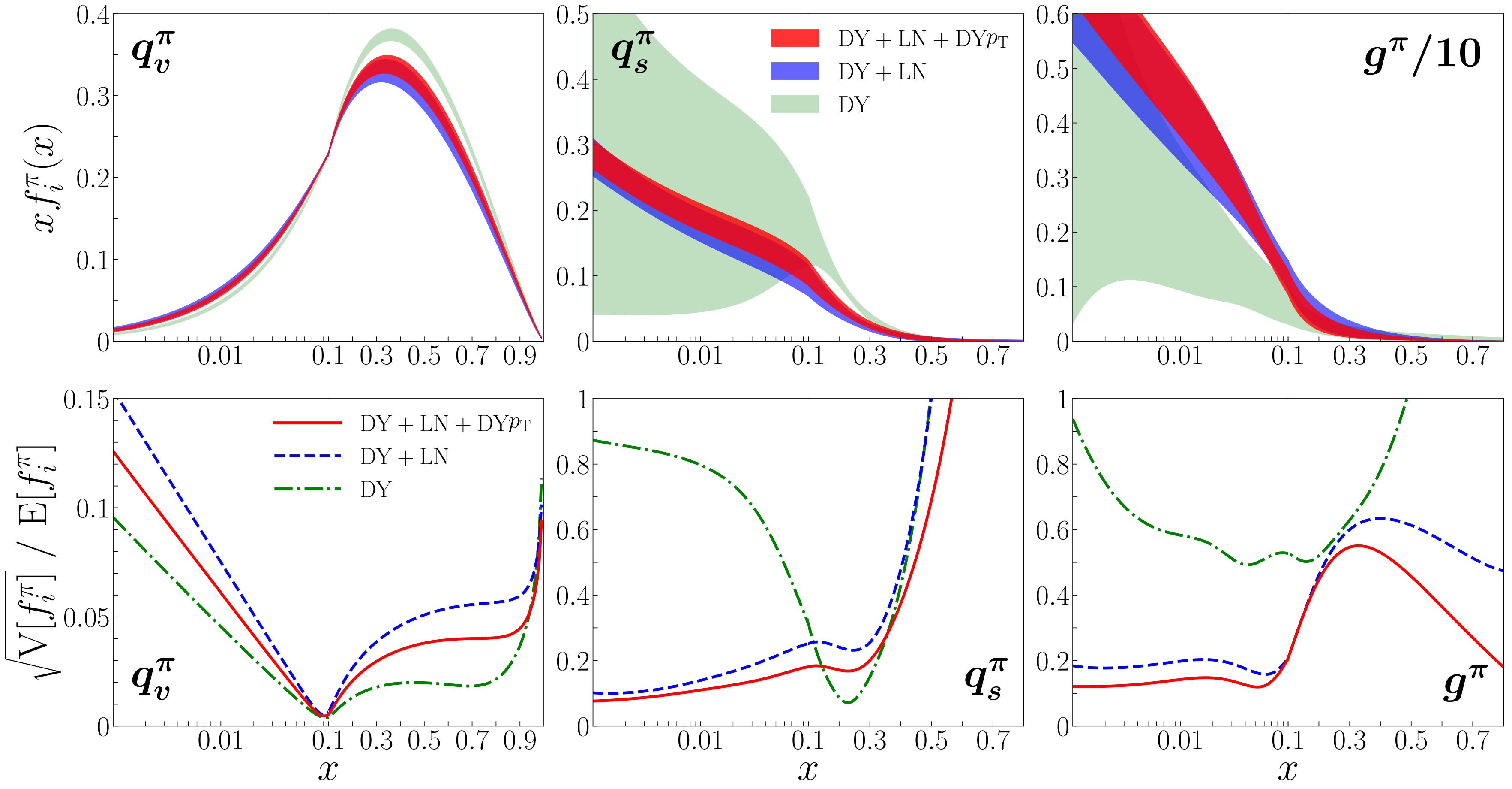

What about the small-q_T?

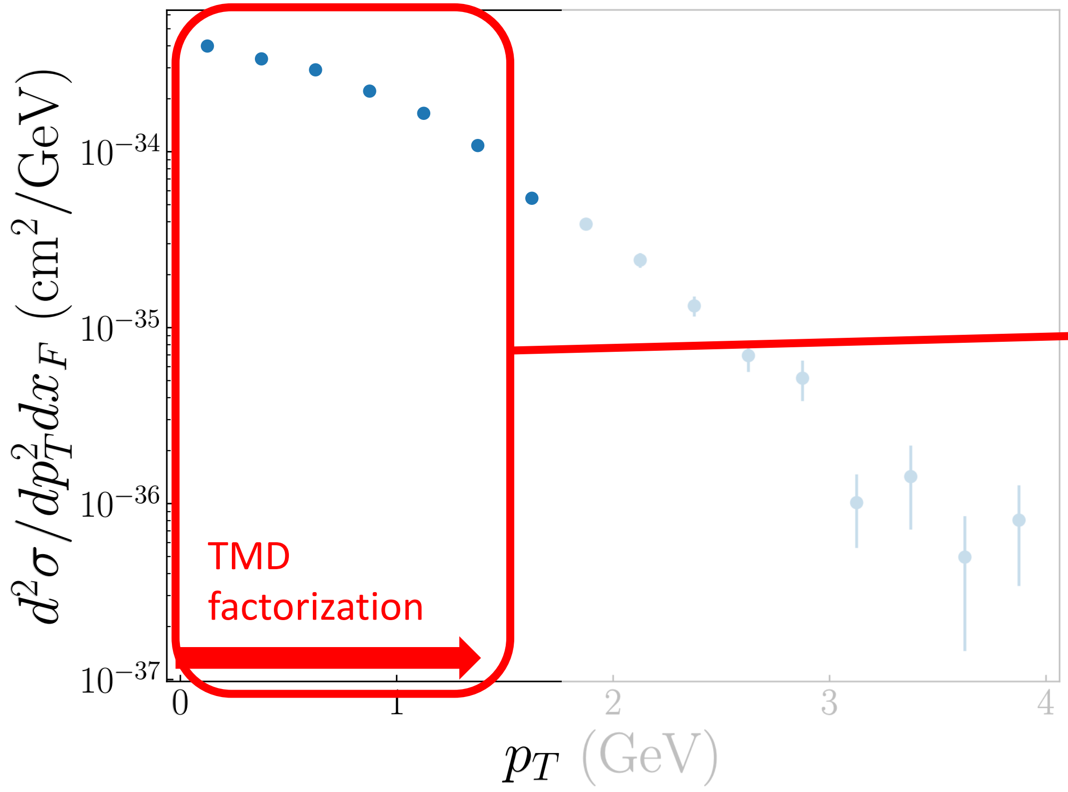

- These data are much more precise
- Can they tell us anything about parton distributions?

The TMD factorization

- Up to now have worked with collinear factorization
- Observables with small-p_T have a different type of factorization theorem – transverse-momentum dependent (TMD) factorization
- In collinear Drell-Yan, we had 2 collinear PDFs convoluted with hard part
    - We extracted π PDFs while assuming the target nuclear PDF
- At small-p_T it is 2 TMDPDFs convoluted with hard part
    - Must parametrize both the π TMDPDF and the target nuclear TMDPDF
- Necessary to understand the nuclear background

Factorization for low-q_T Drell-Yan

- Again, a hard part with two functions that describe structure of beam and target
- So called "W"-term, valid only at low-q_T

$$\frac{d^3\sigma}{d\tau dY dq_T^2} = \frac{4\pi^2\alpha^2}{9\tau S^2} \sum_q H_{q\bar{q}}(Q^2,\mu) \int d^2 b_T\, e^{i b_T \cdot q_T} \times \tilde{f}_{q/\pi}(x_\pi, b_T, \mu, Q^2)\, \tilde{f}_{\bar{q}/A}(x_A, b_T, \mu, Q^2),$$

TMD factorization in Drell-Yan

- In small-q_{T} region, use the Collins-Soper-Sterman (CSS) formalism and b_* prescription

$$b_* = \frac{b_T}{\sqrt{1 + b_T^2/b_{\max}^2}}$$

$$\mu_{b^*} = C_1/b_*$$

$$\begin{aligned}
\frac{\mathrm{d}\sigma}{\mathrm{d}Q^2\,\mathrm{d}y\,\mathrm{d}q_{\mathrm{T}}^2} = \frac{4\pi^2\alpha^2}{9Q^2 s} \sum_{j,j_A,j_B} H_{j\bar{j}}^{\mathrm{DY}}(Q, \mu_Q, a_s(\mu_Q)) \int \frac{\mathrm{d}^2\boldsymbol{b}_{\mathrm{T}}}{(2\pi)^2} e^{i\boldsymbol{q}_{\mathrm{T}}\cdot\boldsymbol{b}_{\mathrm{T}}} \\
\times e^{-g_{j/A}(x_A, b_{\mathrm{T}}; b_{\max})} \int_{x_A}^1 \frac{\mathrm{d}\xi_A}{\xi_A} f_{j_A/A}(\xi_A; \mu_{b_*})\ \tilde{C}_{j/j_A}^{\mathrm{PDF}}\left(\frac{x_A}{\xi_A}, b_*; \mu_{b_*}^2, \mu_{b_*}, a_s(\mu_{b_*})\right) \\
\times e^{-g_{\bar{j}/B}(x_B, b_{\mathrm{T}}; b_{\max})} \int_{x_B}^1 \frac{\mathrm{d}\xi_B}{\xi_B} f_{j_B/B}(\xi_B; \mu_{b_*})\ \tilde{C}_{\bar{j}/j_B}^{\mathrm{PDF}}\left(\frac{x_B}{\xi_B}, b_*; \mu_{b_*}^2, \mu_{b_*}, a_s(\mu_{b_*})\right) \\
\times \exp\left\{-g_K(b_{\mathrm{T}}; b_{\max}) \ln\frac{Q^2}{Q_0^2} + \tilde{K}(b_*; \mu_{b_*}) \ln\frac{Q^2}{\mu_{b_*}^2} + \int_{\mu_{b_*}}^{\mu_Q} \frac{\mathrm{d}\mu'}{\mu'}\left[2\gamma_j(a_s(\mu')) - \ln\frac{Q^2}{(\mu')^2}\gamma_K(a_s(\mu'))\right]\right\}
\end{aligned}$$

TMD factorization in Drell-Yan

- In small-q_{T} region, use the Collins-Soper-Sterman (CSS) formalism and b_* prescription

$$b_* = \frac{b_T}{\sqrt{1 + b_T^2/b_{\max}^2}}$$

$$\mu_{b^*} = C_1/b_*$$

$$\frac{\mathrm{d}\sigma}{\mathrm{d}Q^2\,\mathrm{d}y\,\mathrm{d}q_{\mathrm{T}}^2} = \frac{4\pi^2\alpha^2}{9Q^2 s} \sum_{j,j_A,j_B} H_{j\bar{j}}^{\mathrm{DY}}(Q, \mu_Q, a_s(\mu_Q)) \int \frac{\mathrm{d}^2 \boldsymbol{b}_{\mathrm{T}}}{(2\pi)^2} e^{i\boldsymbol{q}_{\mathrm{T}}\cdot\boldsymbol{b}_{\mathrm{T}}}$$

$$\times\, e^{-g_{j/A}(x_A, b_{\mathrm{T}}; b_{\max})} \int_{x_A}^{1} \frac{\mathrm{d}\xi_A}{\xi_A} f_{j_A/A}(\xi_A; \mu_{b_*})\, \tilde{C}_{j/j_A}^{\mathrm{PDF}}\left(\frac{x_A}{\xi_A}, b_*; \mu_{b_*}^2, \mu_{b_*}, a_s(\mu_{b_*})\right)$$

$$\times\, e^{-g_{\bar{j}/B}(x_B, b_{\mathrm{T}}; b_{\max})} \int_{x_B}^{1} \frac{\mathrm{d}\xi_B}{\xi_B} f_{j_B/B}(\xi_B; \mu_{b_*})\, \tilde{C}_{\bar{j}/j_B}^{\mathrm{PDF}}\left(\frac{x_B}{\xi_B}, b_*; \mu_{b_*}^2, \mu_{b_*}, a_s(\mu_{b_*})\right)$$

$$\times \exp\left\{ -\boxed{g_K}(b_{\mathrm{T}}; b_{\max}) \ln\frac{Q^2}{Q_0^2} + \tilde{K}(b_*; \mu_{b_*}) \ln\frac{Q^2}{\mu_{b_*}^2} + \int_{\mu_{b_*}}^{\mu_Q} \frac{\mathrm{d}\mu'}{\mu'} \left[2\gamma_j(a_s(\mu')) - \ln\frac{Q^2}{(\mu')^2}\gamma_K(a_s(\mu')) \right] \right\}$$

Perturbative pieces

Non-perturbative pieces

Non-perturbative piece of the CS kernel

TMD factorization in Drell-Yan

- In small-q_{T} region, use the Collins-Soper-Sterman (CSS) formalism and b_* prescription

Can these data constrain the pion collinear PDF?

$$\frac{d\sigma}{dQ^2\, dy\, dq_{\mathrm{T}}^2} = \frac{4\pi^2\alpha^2}{9Q^2 s} \sum_{j,j_A,j_B} H^{\mathrm{DY}}_{j\bar{j}}(Q,\mu_Q,a_s(\mu_Q)) \int \frac{d^2\boldsymbol{b}_{\mathrm{T}}}{(2\pi)^2} e^{i\boldsymbol{q}_{\mathrm{T}}\cdot\boldsymbol{b}_{\mathrm{T}}}$$
$$\times\, e^{-g_{j/A}(x_A,b_{\mathrm{T}};b_{\max})} \int_{x_A}^1 \frac{d\xi_A}{\xi_A} \boxed{f_{j_A/A}(\xi_A;\mu_{b_*})}\, \tilde{C}^{\mathrm{PDF}}_{j/j_A}\left(\frac{x_A}{\xi_A}, b_*;\mu_{b_*}^2,\mu_{b_*},a_s(\mu_{b_*})\right)$$
$$\times\, e^{-g_{\bar{j}/B}(x_B,b_{\mathrm{T}};b_{\max})} \int_{x_B}^1 \frac{d\xi_B}{\xi_B} f_{j_B/B}(\xi_B;\mu_{b_*})\, \tilde{C}^{\mathrm{PDF}}_{\bar{j}/j_B}\left(\frac{x_B}{\xi_B}, b_*;\mu_{b_*}^2,\mu_{b_*},a_s(\mu_{b_*})\right)$$
$$\times \exp\left\{-\boxed{g_K}(b_{\mathrm{T}};b_{\max}) \ln\frac{Q^2}{Q_0^2} + \tilde{K}(b_*;\mu_{b_*}) \ln\frac{Q^2}{\mu_{b_*}^2} + \int_{\mu_{b_*}}^{\mu_Q} \frac{d\mu'}{\mu'}\left[2\gamma_j(a_s(\mu')) - \ln\frac{Q^2}{(\mu')^2}\gamma_K(a_s(\mu'))\right]\right\}$$

Perturbative pieces

Non-perturbative pieces

Non-perturbative piece of the CS kernel

Nuclear TMDPDFs

- The TMD-factorization allows for the description of a quark inside a nucleus to be $\tilde{f}_{q/A}$
- However, the intrinsic non-perturbative structure will in-principle change from nucleus-to-nucleus
- Want to model these in terms of protons and neutrons as we don't have enough observables to separately parametrize different nuclei

Nuclear TMDPDFs – working hypothesis

- We must model the tungsten TMDPDF from proton

$$\tilde{f}_{q/A}(x, b_T, \mu, \zeta) = \frac{Z}{A} \tilde{f}_{q/p/A}(x, b_T, \mu, \zeta) + \frac{A-Z}{A} \tilde{f}_{q/n/A}(x, b_T, \mu, \zeta)$$

- Each object on the right side independently obeys the CSS equation
  - **Assumption** that the bound proton and bound neutron follow TMD factorization
- Make use of isospin symmetry in that $u/p/A \leftrightarrow d/n/A$, etc.

Building of the nuclear TMDPDF

- Then taking into account the intrinsic non-perturbative, we model the flavor-dependent pieces of the TMDPDF as

$$
\begin{aligned}
(C\otimes f)_{u/A}(x)e^{-g_{u/A}(x,b_T)} \to\ & \frac{Z}{A}(C\otimes f)_{u/p/A}(x)e^{-g_{u/p/A}(x,b_T)} \\
&+\frac{A-Z}{A}(C\otimes f)_{d/p/A}(x)e^{-g_{d/p/A}(x,b_T)}
\end{aligned}
$$

and

$$
\begin{aligned}
(C\otimes f)_{d/A}(x)e^{-g_{d/A}(x,b_T)} \to\ & \frac{Z}{A}(C\otimes f)_{d/p/A}(x)e^{-g_{d/p/A}(x,b_T)} \\
&+\frac{A-Z}{A}(C\otimes f)_{u/p/A}(x)e^{-g_{u/p/A}(x,b_T)}.
\end{aligned}
$$

Datasets in the analysis

Expt.	$\sqrt{s}$ (GeV)	Reaction	Observable	Q (GeV)	x_F or y	$N_{\text{pts.}}$
E288 [39]	19.4	$p + Pt \to \ell^+\ell^- X$	$Ed^3\sigma/d^3\mathbf{q}$	$4 - 9$	$y = 0.4$	38
E288 [39]	23.8	$p + Pt \to \ell^+\ell^- X$	$Ed^3\sigma/d^3\mathbf{q}$	$4 - 12$	$y = 0.21$	48
E288 [39]	24.7	$p + Pt \to \ell^+\ell^- X$	$Ed^3\sigma/d^3\mathbf{q}$	$4 - 14$	$y = 0.03$	74
E605 [40]	38.8	$p + Cu \to \ell^+\ell^- X$	$Ed^3\sigma/d^3\mathbf{q}$	$7 - 18$	$x_F = 0.1$	49
E772 [41]	38.8	$p + D \to \ell^+\ell^- X$	$Ed^3\sigma/d^3\mathbf{q}$	$5 - 15$	$0.1 \leq x_F \leq 0.3$	61
E866 [50]	38.8	$p + Fe \to \ell^+\ell^- X$	R_{FeBe}	$4 - 8$	$0.13 \leq x_F \leq 0.93$	10
E866 [50]	38.8	$p + W \to \ell^+\ell^- X$	R_{WBe}	$4 - 8$	$0.13 \leq x_F \leq 0.93$	10
E537 [38]	15.3	$\pi^- + W \to \ell^+\ell^- X$	$d^2\sigma/dx_F dq_T$	$4 - 9$	$0 < x_F < 0.8$	48
E615 [4]	21.8	$\pi^- + W \to \ell^+\ell^- X$	$d^2\sigma/dx_F dq_T^2$	$4.05 - 8.55$	$0 < x_F < 0.8$	45

- Total of 383 number of points
- All fixed target, low-energy data

Kinematics in x_1, x_2

- Using the kinematic mid-point from each of the bins, we show the range in x_1 and x_2

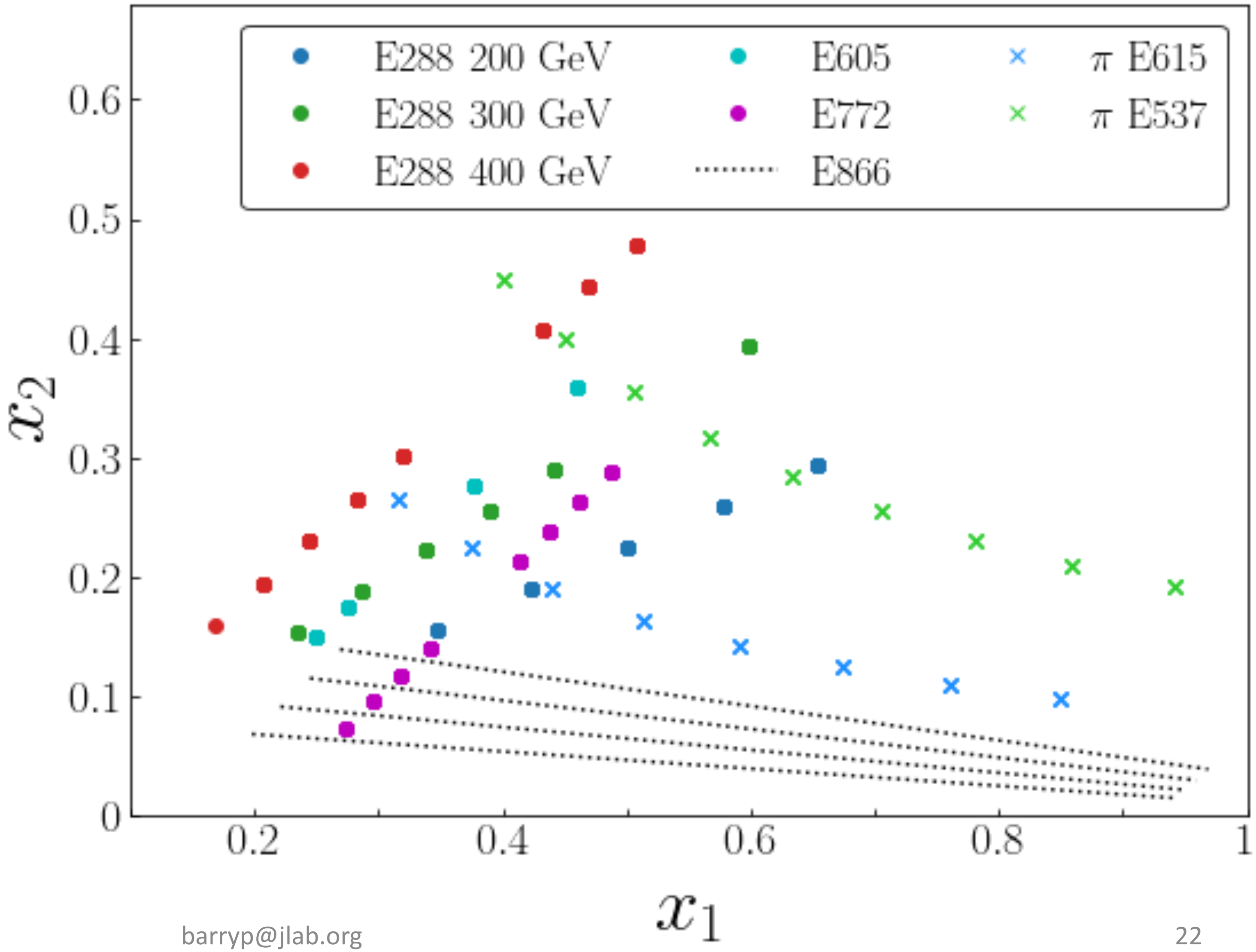

Parametrizations of the TMDs

- First perform single fits of these data to explore various aspects
- Many types of parametrizations have been used in the past
- For the “intrinsic” non-perturbative TMD, we perform fits with each of the following

Gaussian

$$\exp(-g_{q/N}(x, b_T)) = \exp\left(-g_q(x, A)\, b_T^2\right) ,$$

Exponential

$$\exp(-g_{q/N}(x, b_T)) = \exp\left(-g_q(x, A)\, b_T\right) ,$$

Gaussian-to-Exponential

$$\exp(-g_{q/N}(x, b_T)) = \exp\left(-g_q(x, A)\, \frac{b_T^2}{\sqrt{1 + B_{NP}(x) b_T^2}}\right) ,$$

Parametrizations

- We can test whether or not the x-dependence is important for these functions (it is!)
- For these g_q functions, we have the following

$$g_q(x,A) = |g^q + g_2^q x + g_3^q (1-x)^2|(1 + g_1(A^{1/3} - 1)) \ ,$$
$$B_{NP}(x) = b_{NP} x^2 \ ,$$

- 4 free parameters for each scheme (5 for Gaussian-to-Exponential)
- We may also open up these for each flavor in the proton (u, d, and sea) and for the pion (val, sea)

Problem describing data

- The E288 400 GeV data are difficult to describe the same above and below the Υ resonance
- Theory overpredicts data when $Q > 11\text{GeV}$

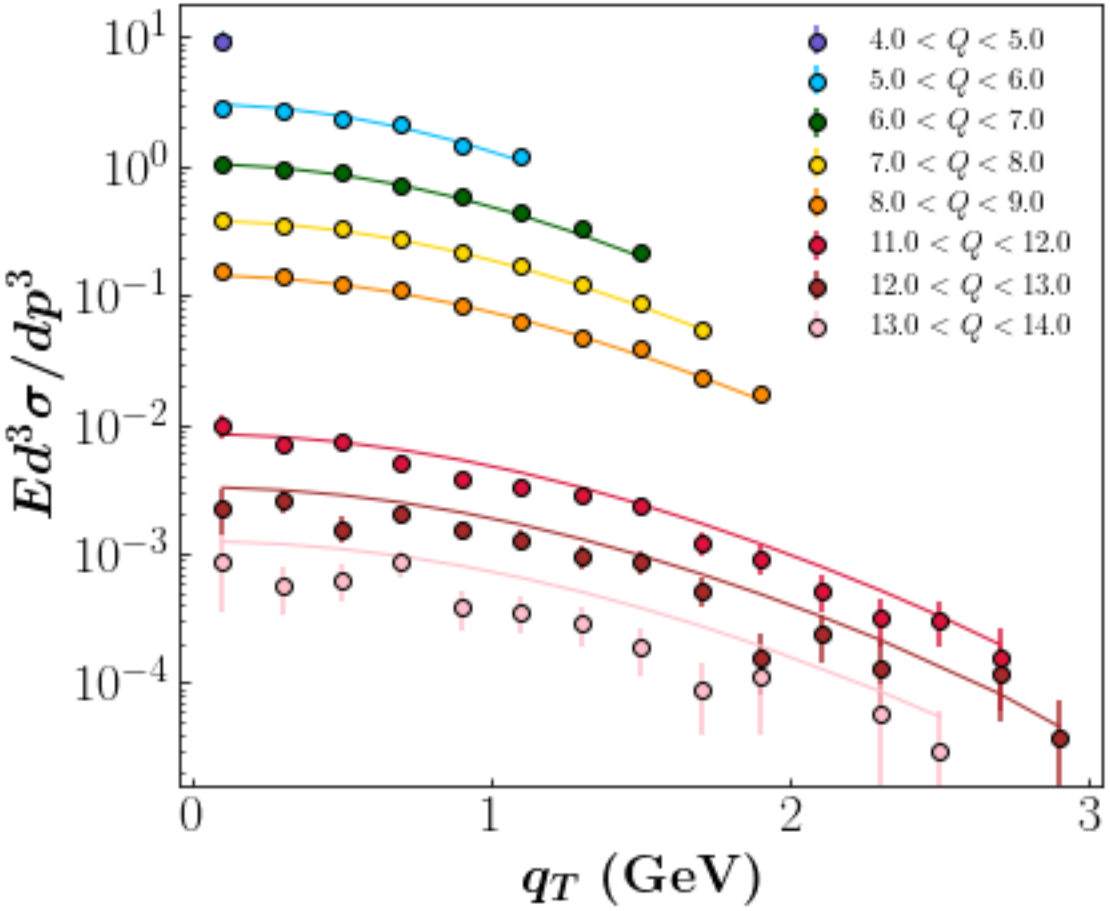

Problem describing data

- The E288 400 GeV data are difficult to describe the same above and below the Υ resonance
- Theory overpredicts data when $Q > 11\text{GeV}$
- Could treat as separate datasets – separate normalizations:

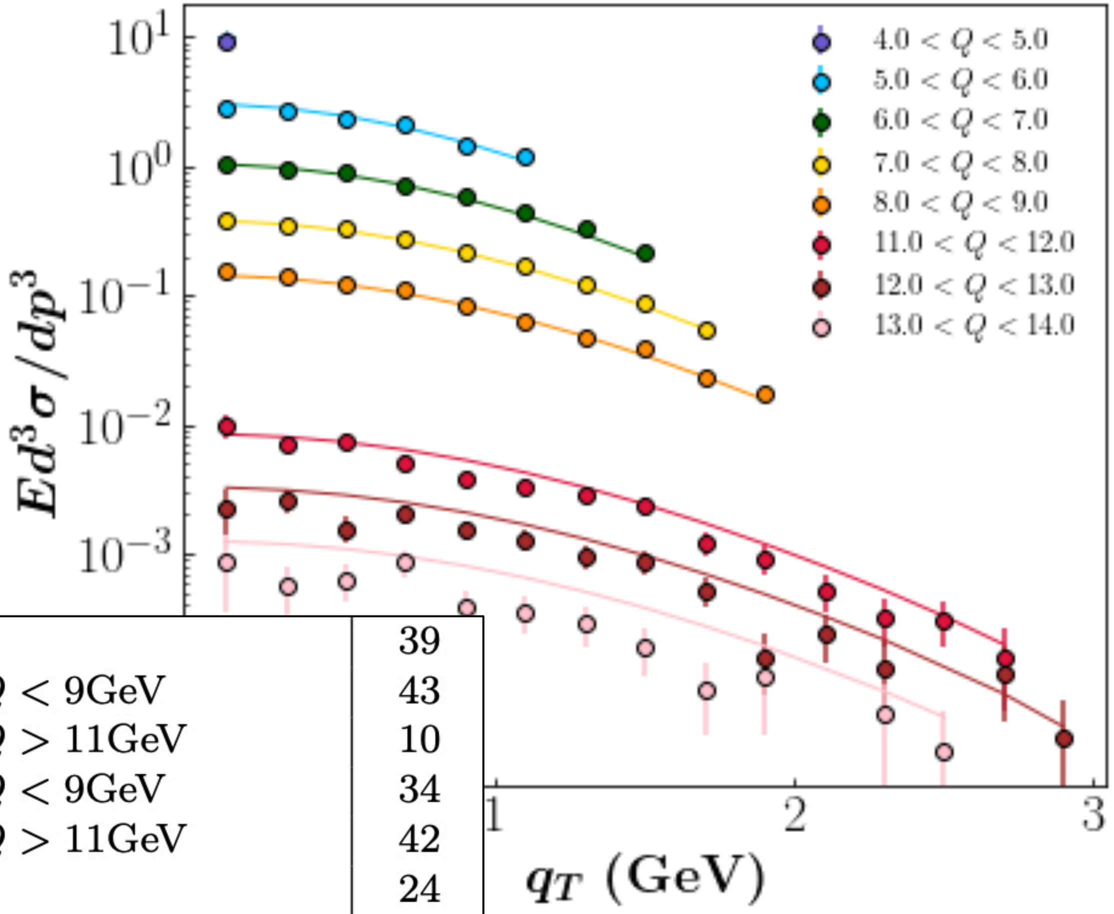

E228-200	39
E228-300 $Q < 9\text{GeV}$	43
E228-300 $Q > 11\text{GeV}$	10
E228-400 $Q < 9\text{GeV}$	34
E228-400 $Q > 11\text{GeV}$	42
E772	24
E605 $Q < 9\text{GeV}$	21
E605 $Q > 11\text{GeV}$	32

MAP parametrization

- A recent work from the MAP collaboration (arXiv:2206.07598) used a complicated form for the non-perturbative function

$$f_{1\,NP}(x, \boldsymbol{b}_T^2; \zeta, Q_0) = \frac{g_1(x)\, e^{-g_1(x)\frac{\boldsymbol{b}_T^2}{4}} + \lambda^2\, g_{1B}^2(x) \left[1 - g_{1B}(x)\frac{\boldsymbol{b}_T^2}{4}\right] e^{-g_{1B}(x)\frac{\boldsymbol{b}_T^2}{4}} + \lambda_2^2\, g_{1C}(x)\, e^{-g_{1C}(x)\frac{\boldsymbol{b}_T^2}{4}}}{g_1(x) + \lambda^2\, g_{1B}^2(x) + \lambda_2^2\, g_{1C}(x)} \left[\frac{\zeta}{Q_0^2}\right]^{\boxed{g_K(\boldsymbol{b}_T^2)/2}}, \quad (38)$$

$$g_{\{1,1B,1C\}}(x) = N_{\{1,1B,1C\}} \frac{x^{\sigma_{\{1,2,3\}}} (1-x)^{\alpha^2_{\{1,2,3\}}}}{\hat{x}^{\sigma_{\{1,2,3\}}} (1-\hat{x})^{\alpha^2_{\{1,2,3\}}}},$$

$$\boxed{g_K(\boldsymbol{b}_T^2) = -g_2^2 \frac{\boldsymbol{b}_T^2}{2}}$$

Universal CS kernel

- 11 free parameters for each hadron! (flavor dependence not necessary) (12 if we include the nuclear TMD parameter)

Resulting χ^2 for each parametrization

- MAP gives best overall
- How significant?

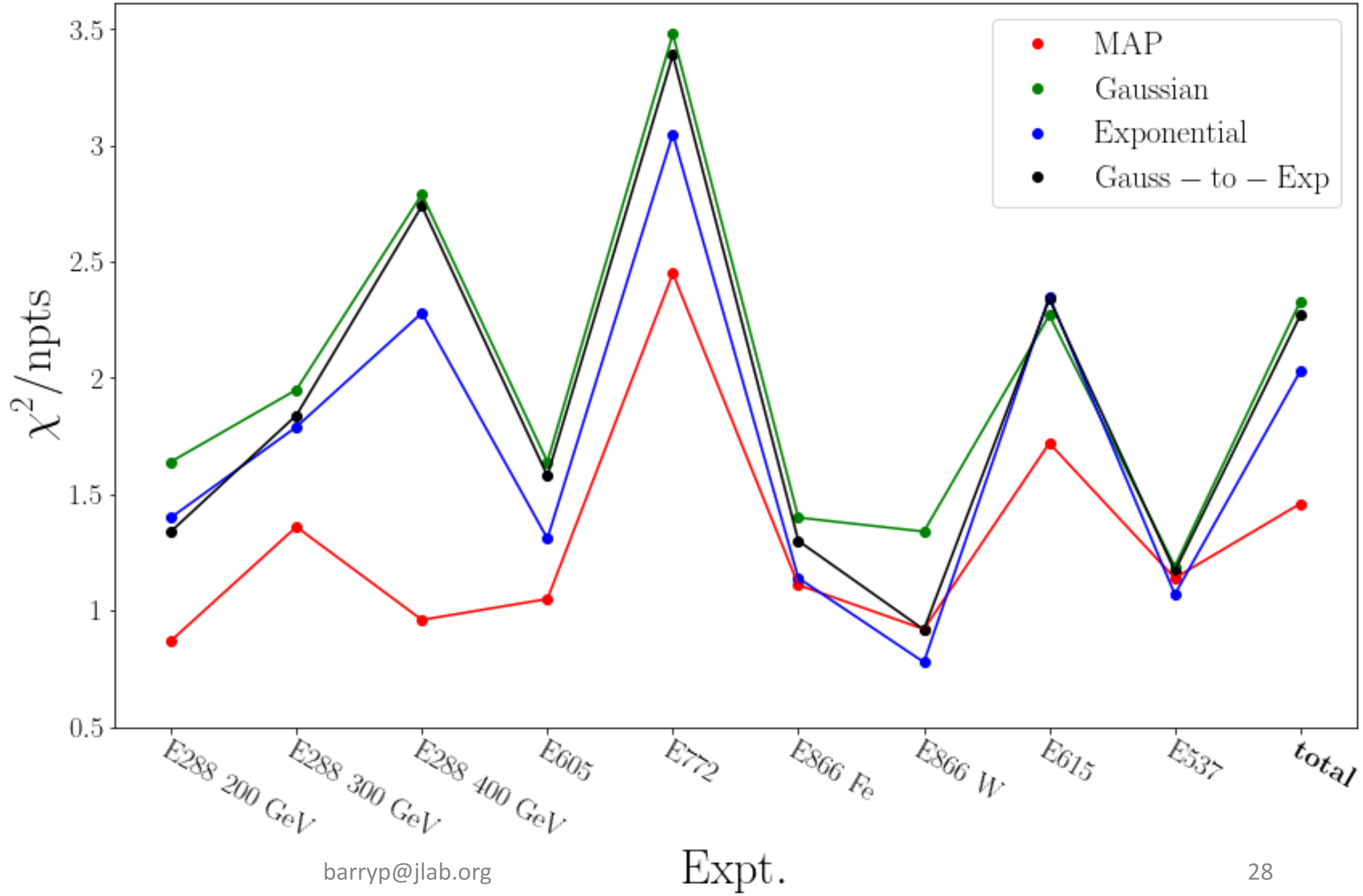

E772 data

- Let’s take a look at the data and theory agreement
- Data do not always follow the general trend and uncertainties appear underestimated

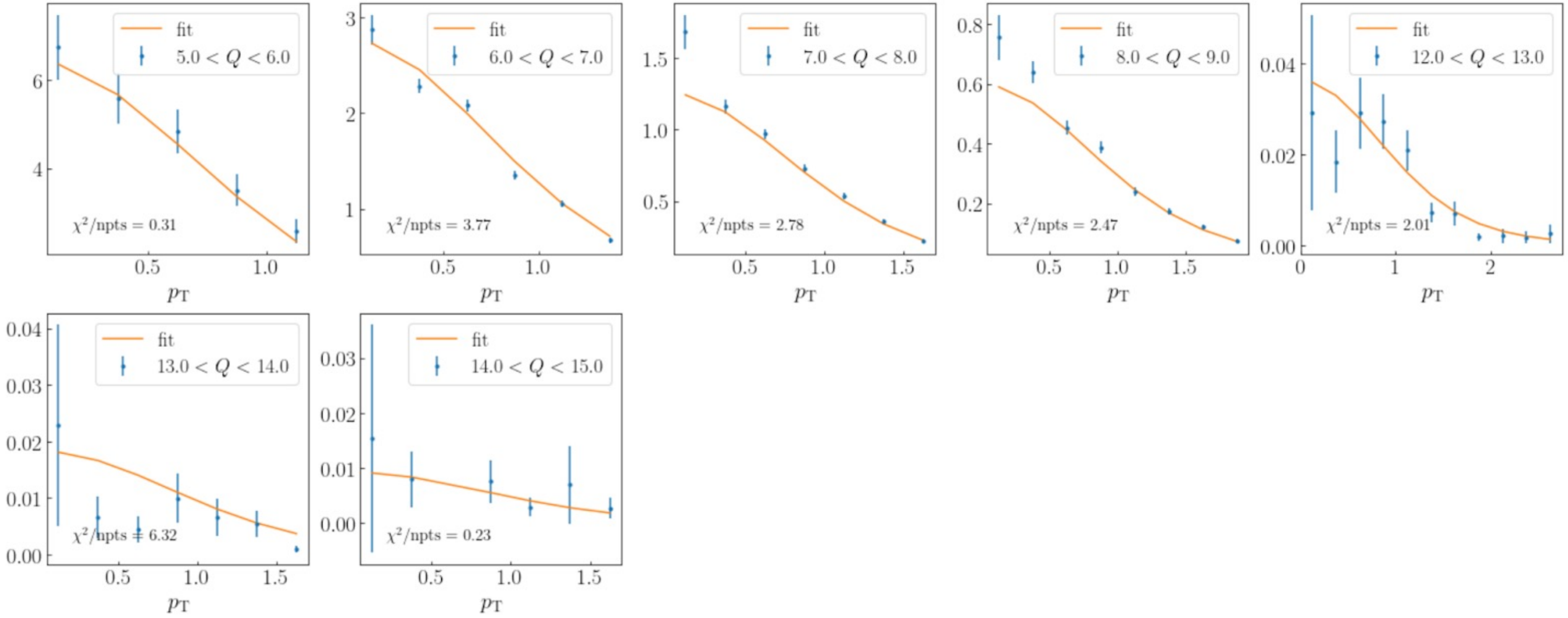

A few words on nuclear dependence

- The ratios from the E866 experiment provided a look to nuclear effects in TMDs as well as the importance of nuclear collinear effects
- Ignoring any nuclear corrections in TMDs and collinear PDFs

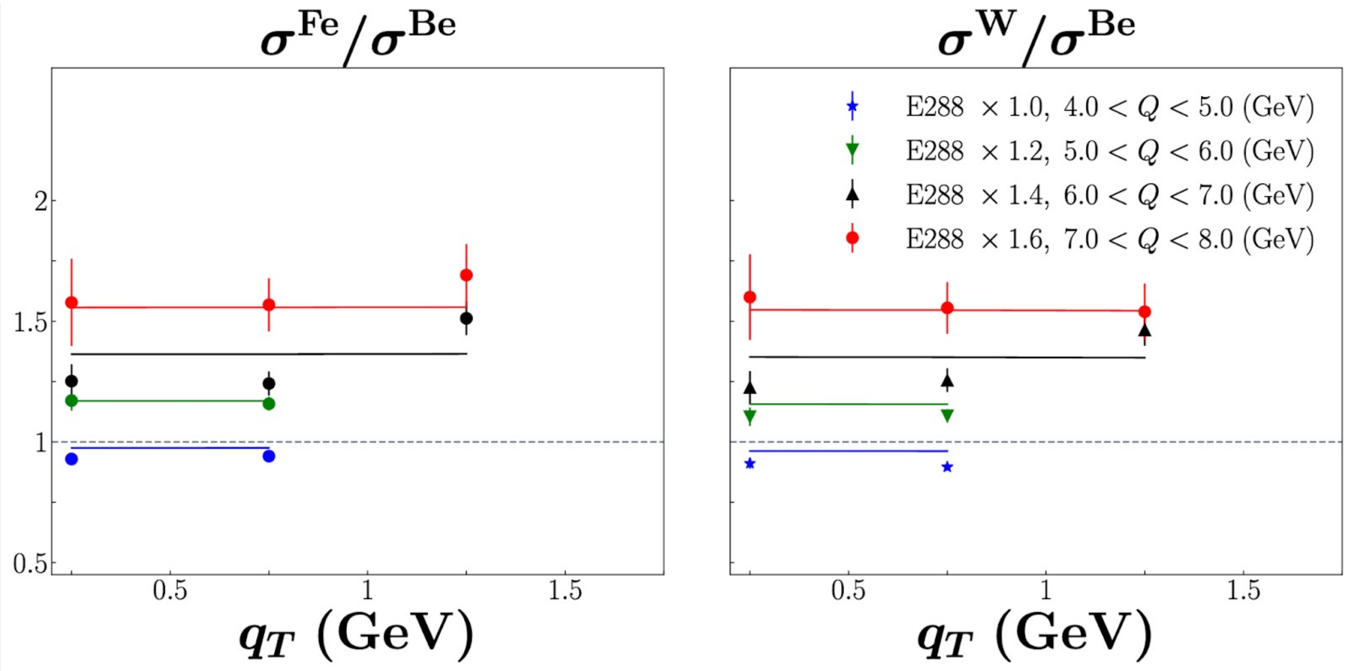

col	obs	tar	npts	chi2/npts	Z-score
E866	ratio	Fe/Be	10	2.2	2.16
E866	ratio	W/Be	10	3.51	3.67

Including nuclear dependence

- Better description when including the nuclear dependence in the collinear PDF and TMD

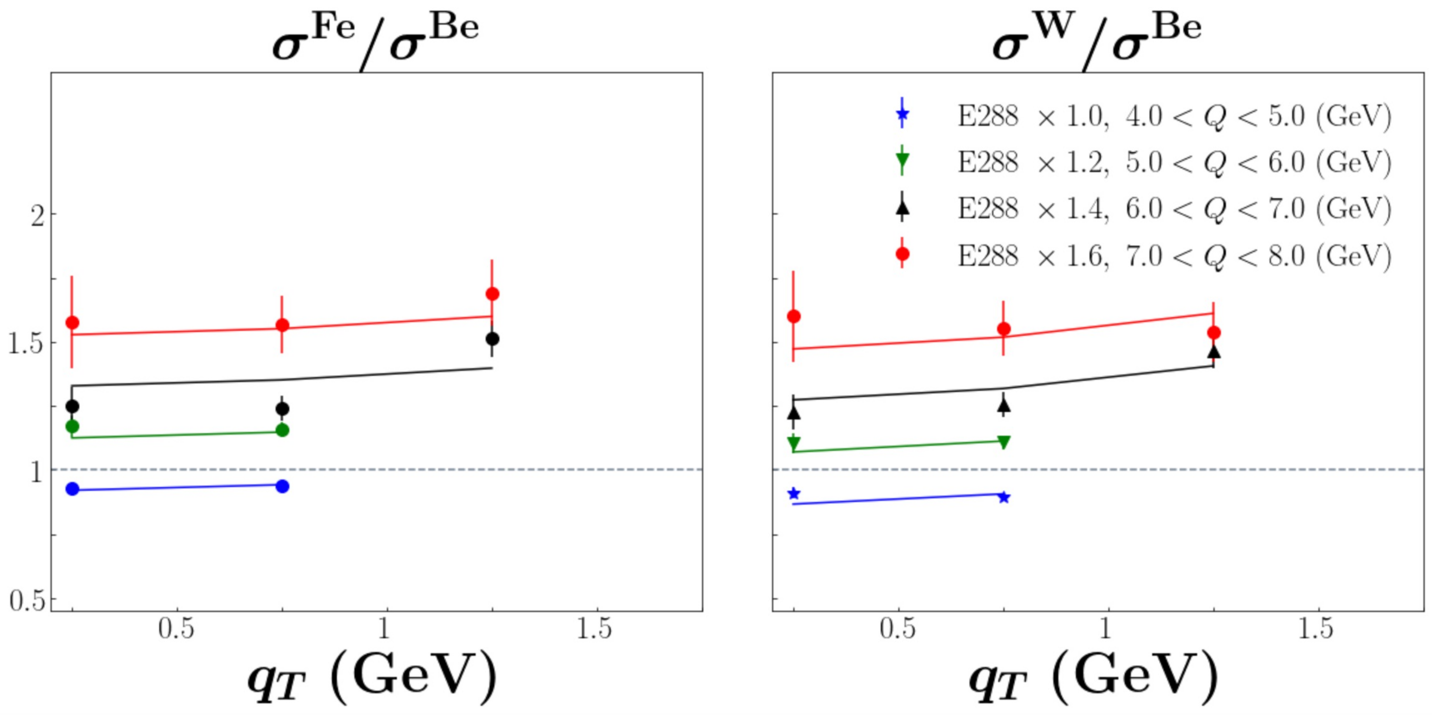

col	obs	tar	npts	chi2/npts	Z-score
E866	ratio	Fe/Be	10	1.11	0.4
E866	ratio	W/Be	10	0.92	0.04

Strategy

- Given our single fits, we will freeze the proton (nuclear) TMD and open up pion PDF parameters
- Perform a simultaneous fit of both pion PDF and TMDPDF parameters
- Use the MAP parametrization

Description of πA data

- Well describe the E615 data in the (x_F, q_T) spectrum: $\chi^2/\text{npts} = 1.63$
- Can also describe rest of the experimental data: $\chi^2_{\text{tot}}/\text{npts} = 0.98$
- Overall Z-score= 0.62

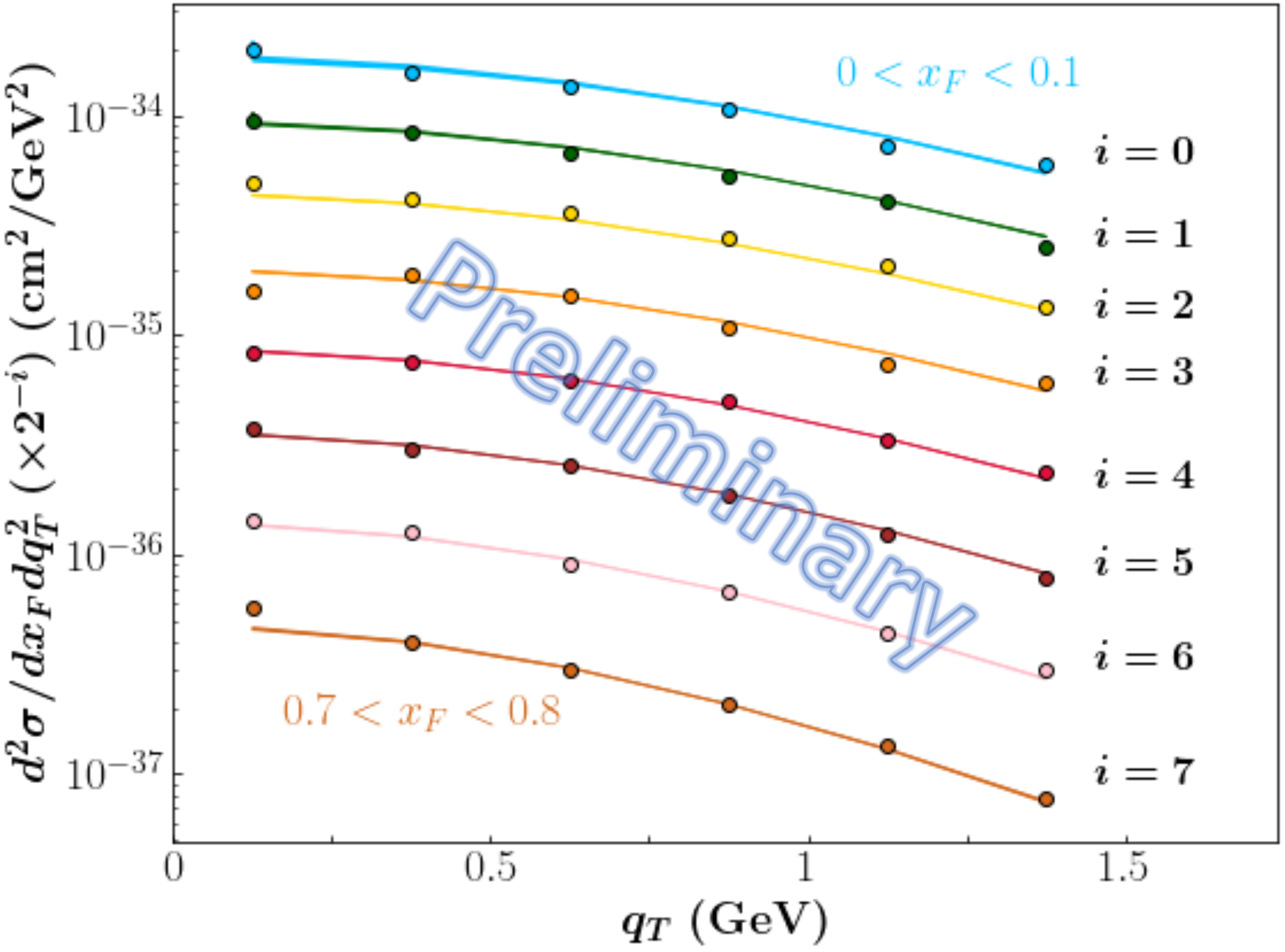

Impact on PDFs

- Slight reduction in uncertainties
- Overall very consistent with totally collinear analysis

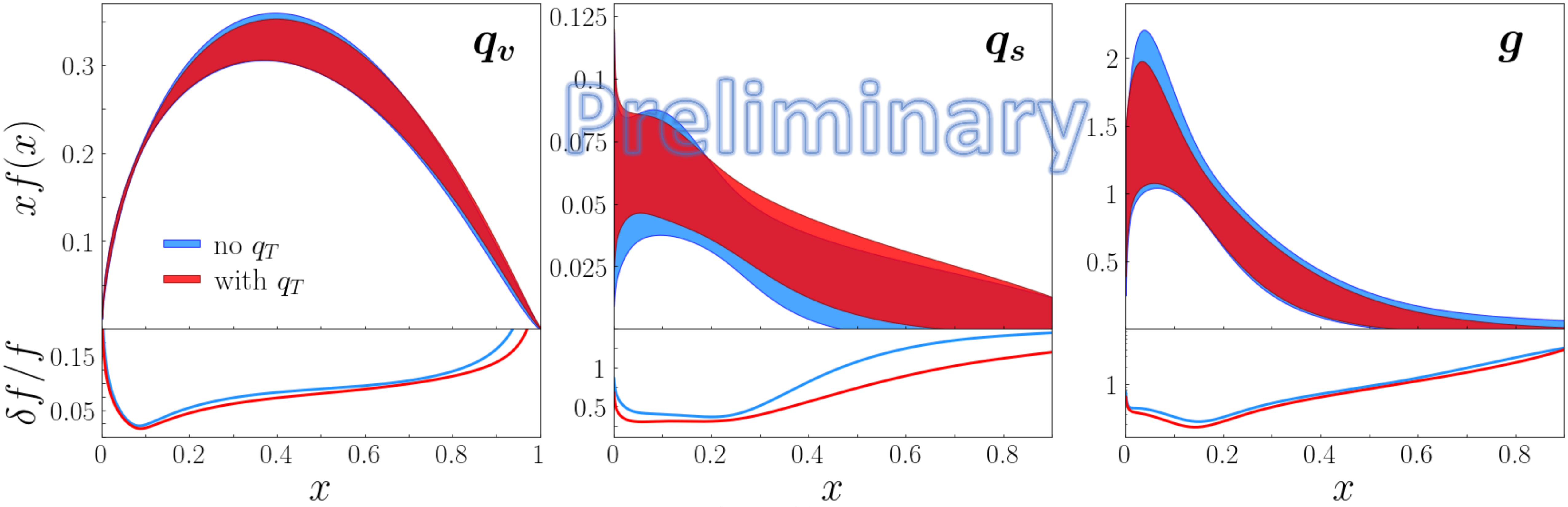

Future extension: Can LHC constrain PDFs?

- From Bury, et al. arXiv:2201.07114

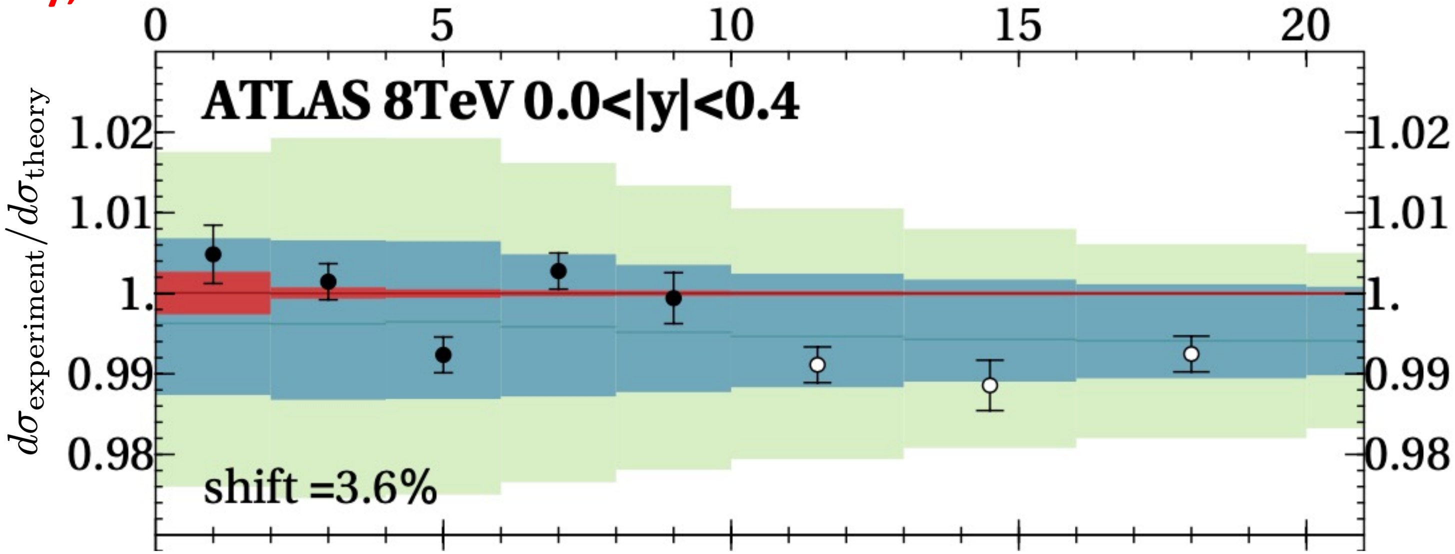

- The outer green band is the uncertainty from MSHT20 PDFs
- Red band is the statistical uncertainty from the data
- Largest uncertainty comes from PDF itself!

What about the entire q_T-spectrum?

- The JAM collaboration has shown the ability to perform a global analysis separately of the large-q_T and small- q_T regions
- Tackle the challenging "asymptotic region"
- Can we combine these analyses in the π-sector?

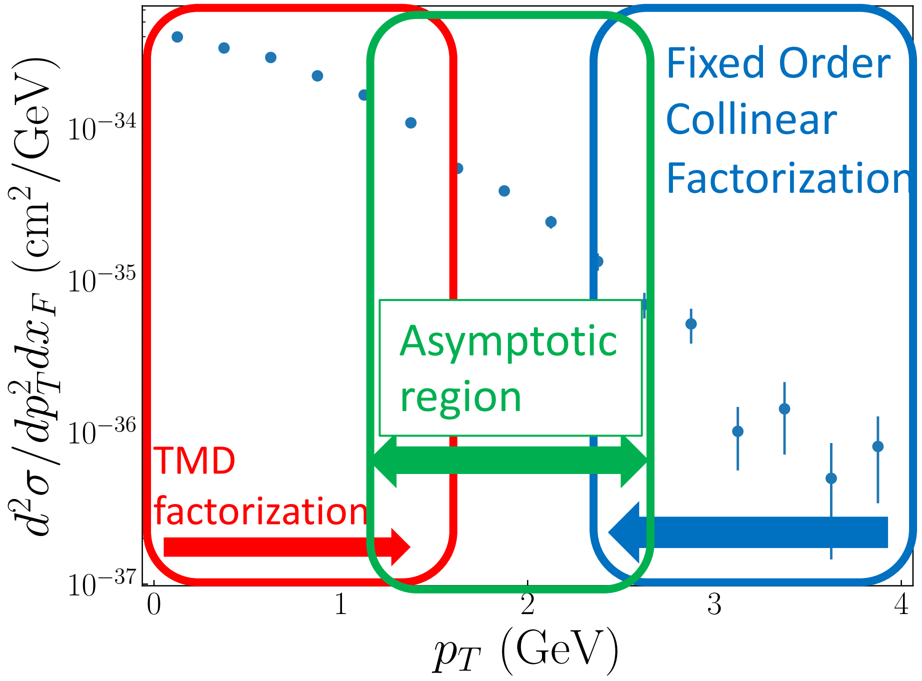

Conclusions

- We have made strides in collinear pion PDF phenomenology by introducing available datasets and theoretical advances
- Inclusion of q_T-dependent DY data is consistent with collinear data
- Next step to analyze MC on πA and pA data combined
    - Get statistical uncertainty on CS kernel
- Extend framework to LHC data and nucleon PDFs

Backup Slides

Two-hadron $\widetilde{K}$ extractions

- The Collins-Soper kernel is the most universal quantity in TMD physics
- No dependence on flavor, species, or type of TMD
- Extracted from single fit to both pA and πA data
- Green lattice points from Shanahan, et al., Phys. Rev. D **104**, 114502 (2021)

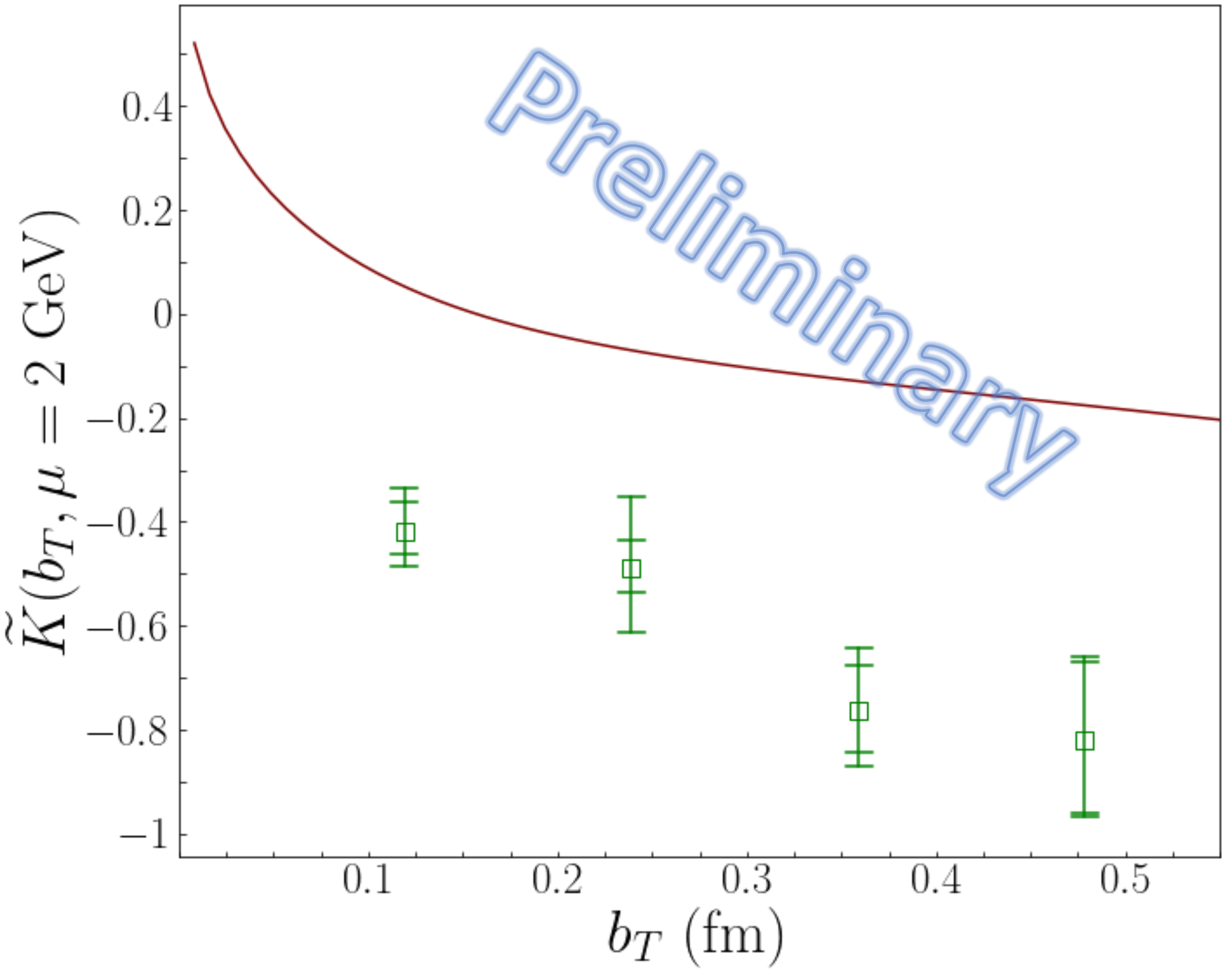

Fitting the Data and Systematic Corrections

Valence quark distribution in pion

Wilson coefficients for matching

$$\mathrm{Re}\,\mathfrak{M}(\nu, z^2) = \int_0^1 \mathrm{d}x\, \boxed{q_v(x, \mu_{\mathrm{lat}})}\, \boxed{\mathcal{C}^{\mathrm{Rp-ITD}}\left(x\nu, z^2, \mu_{\mathrm{lat}}\right)} + \boxed{z^2 B_1(\nu)} + \boxed{\frac{a}{|z|} P_1(\nu)} + \boxed{e^{-m_\pi (L-z)} F_1(\nu)} + \boxed{\ldots}$$

Integration lower bound is 0

Other potential systematic corrections the data is not sensitive to

<u>Systematic corrections to parametrize</u>

- $z^2 B_1(\nu)$: power corrections
- $\frac{a}{|z|} P_1(\nu)$: lattice spacing errors
- $e^{-m_\pi (L-z)} F_1(\nu)$: finite volume corrections

Evolution equations for the TMDPDF

$$\frac{\partial \ln \tilde{f}_{f/H}(x, b_{\mathrm{T}}; \zeta; \mu)}{\partial \ln \sqrt{\boxed{\zeta}}} = \boxed{\tilde{K}(b_{\mathrm{T}}; \mu).}$$

Collins-Soper (CS) kernel

Rapidity scale

Has its own renormalization group equation

$$\frac{\mathrm{d}\tilde{K}(b_{\mathrm{T}}; \mu)}{\mathrm{d}\ln\mu} = \boxed{-\gamma_K(a_s(\mu))}$$

Anomalous dimension of CS kernel

$$\frac{\mathrm{d}\ln \tilde{f}_{j/H}(x, b_{\mathrm{T}}; \zeta; \mu)}{\mathrm{d}\ln \boxed{\mu}} = \boxed{\gamma_j(a_s(\mu))} - \frac{1}{2}\boxed{\gamma_K(a_s(\mu))}\ln\frac{\zeta}{\mu^2},$$

Renormalization scale

Anomalous dimension of TMDPDF

Small b_T operator product expansion

- At small b_T, the TMDPDF can be described in terms of its OPE:

$$\tilde{f}_{j/H}(x, b_{\mathrm{T}}; \zeta; \mu) = \sum_k \int_{x-}^{1+} \frac{\mathrm{d}\xi}{\xi} \, \tilde{C}^{\mathrm{PDF}}_{j/k}(x/\xi, b_{\mathrm{T}}; \zeta, \mu, a_s(\mu)) \, f_{k/H}(\xi; \mu) \; + \; O[(m b_{\mathrm{T}})^p] \, .$$

- where $\tilde{C}$ are the Wilson coefficients, and $f_{j/P}$ is the collinear PDF
- Breaks down when b_T gets large
- NB: the scale μ appears both in $\tilde{C}$ and $f_{j/P}$

Scale choice

- We see for instance the Wilson coefficients up to $\mathcal{O}(\alpha_S)$

$$\tilde{C}_{j'/j}(x, \mathbf{b}_T; \mu; \zeta_F/\mu^2) = \delta_{j'j}\delta(1-x) + \delta_{j'j}\frac{\alpha_s C_\mathrm{F}}{2\pi}\left\{2\left[\ln\left(\frac{2}{\mu b_\mathrm{T}}\right) - \gamma_\mathrm{E}\right]\left[\left(\frac{2}{1-x}\right)_+ - 1 - x\right] + 1 - x + \right.$$
$$\left. + \delta(1-x)\left[-\frac{1}{2}\left[\ln\left(b_\mathrm{T}^2\mu^2\right) - 2(\ln 2 - \gamma_\mathrm{E})\right]^2 - \left[\ln(b_\mathrm{T}^2\mu^2) - 2(\ln 2 - \gamma_\mathrm{E})\right]\ln\left(\frac{\zeta_F}{\mu^2}\right)\right]\right\} + \mathcal{O}(\alpha_s^2).$$

- We should choose a scale to maintain the perturbative accuracy
- Convenient choice: $\mu = \frac{C_1}{b_T}$, where $C_1 = 2e^{-\gamma_E}$
- *However*, at large b_T, the scale becomes too small to trust the factorization

b_* prescription

- A common approach to regulating large b_T behavior

$$\mathbf{b}_*(\mathbf{b}_T) \equiv \frac{\mathbf{b}_T}{\sqrt{1 + b_T^2/b_{\max}^2}}.$$

Must choose an appropriate value; a transition from perturbative to non-perturbative physics

- At small b_T, $b_*(b_T) = b_T$
- At large $b_T, b_*(b_T) = b_{\max}$
- Here, the renormalization scale is evaluated at

$$\mu_b = \frac{C_1}{b_*(\mathbf{b}_T)}.$$

- This cancels all logarithms when $C_1 = 2e^{-\gamma_E}$

Introduction of non-perturbative functions

- Because $b_* \neq b_T$, have to non-perturbatively describe large b_T behavior

Completely general – independent of quark, hadron, PDF or FF

"Holy grail" in TMD pheno

$$g_K(b_\mathrm{T}; b_\mathrm{max}) = -\tilde{K}(b_\mathrm{T}, \mu) + \tilde{K}(b_*, \mu)$$

Non-perturbative function dependent in principle on flavor, hadron, etc.

$$e^{-g_{j/H}(x, \boldsymbol{b}_\mathrm{T}; b_\mathrm{max})} = \frac{\tilde{f}_{j/H}(x, \boldsymbol{b}_\mathrm{T}; \zeta, \mu)}{\tilde{f}_{j/H}(x, \boldsymbol{b}_*; \zeta, \mu)} e^{g_K(b_\mathrm{T}; b_\mathrm{max}) \ln(\sqrt{\zeta}/Q_0)}.$$

Treatment of nuclear TMDPDFs

- We want to make use of knowledge of nuclear effects on the collinear side

$$f_{u/p/A}(x,\mu) = \frac{Z}{2Z-A} f_{u/A}(x,\mu) + \frac{Z-A}{2Z-A} f_{d/A}(x,\mu)$$

and

$$f_{d/p/A}(x,\mu) = \frac{Z}{2Z-A} f_{d/A}(x,\mu) + \frac{Z-A}{2Z-A} f_{u/A}(x,\mu) \, .$$

- Where $f_{u/A}(x,\mu)$, etc. is reported by EPPS16
- These formulas are also used for the corresponding antiquarks

Bayesian Inference

- Minimize the χ^2

Normalization parameter

$$\chi^2(\boldsymbol{a},\mathrm{data}) = \sum_e \left(\sum_i \left[\frac{d_i^e - \sum_k r_k^e \beta_{k,i}^e - t_i^e(\boldsymbol{a})/n_e}{\alpha_i^e} \right]^2 + \left(\frac{1-n_e}{\delta n_e} \right)^2 + \sum_k \left(r_k^e \right)^2 \right)$$

Perturbative orders

- We use NLO+N^{2}LL perturbative accuracy

Function	Order
H	$\mathcal{O}(\alpha_S)$
$\tilde{C}^{\mathrm{PDF}}$	$\mathcal{O}(\alpha_S)$
K and γ_F	$\mathcal{O}(\alpha_S^2)$
γ_K	$\mathcal{O}(\alpha_S^3)$

- But where are expansions appropriate?
- Consider the fixed order pieces:
  - Can multiply out each contribution
  - Can truncate to only accuracy by each piece

$$\sigma \propto H \ \mathrm{OPE}_A \ \mathrm{OPE}_B$$
$$\approx (1+\alpha_S \hat{H})(1+\alpha_S \widehat{\mathrm{OPE}}_A)(1+\alpha_S \widehat{\mathrm{OPE}}_B)$$
$$\approx 1+\alpha_S(\hat{H}+\widehat{\mathrm{OPE}}_A+\widehat{\mathrm{OPE}}_B)+\mathcal{O}(\alpha_S^2)$$

Z-scores

- A measure of significance with respect to the normal distribution
- Null hypothesis is the expected χ^2 distribution

$$Z = \Phi^{-1}(p) \equiv \sqrt{2}\,\mathrm{erf}^{-1}(2p - 1).$$

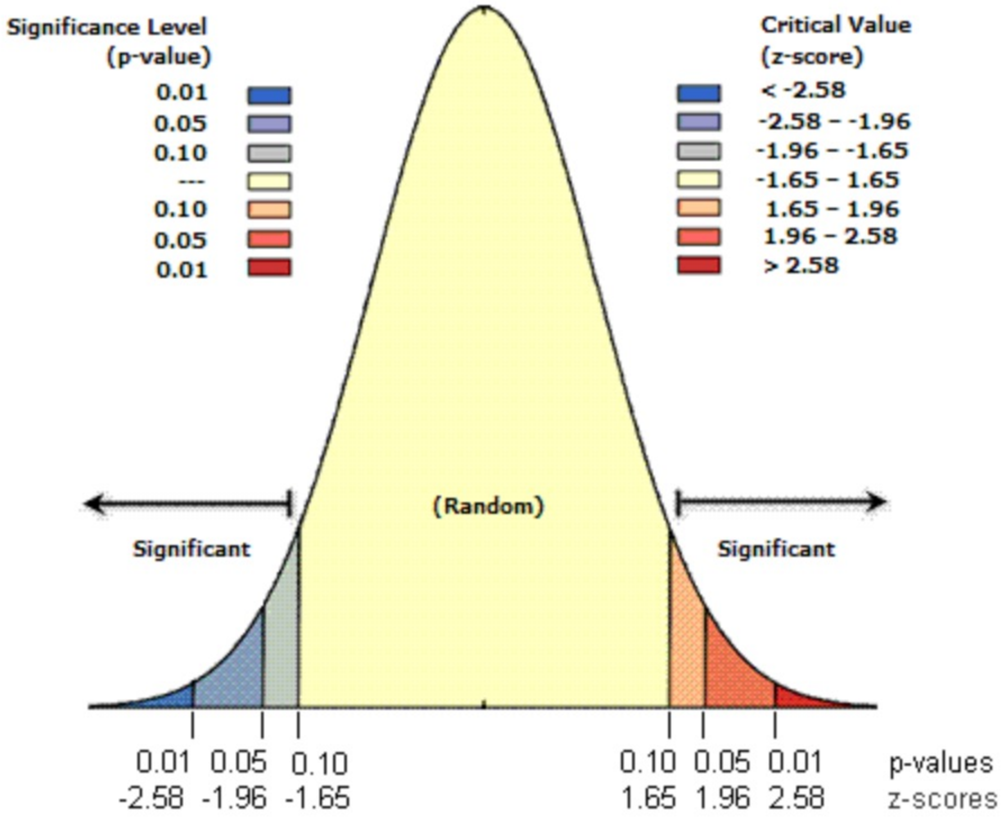

Z-scores

- Example of significance of the χ^2 values with respect to the expected χ^2 distribution

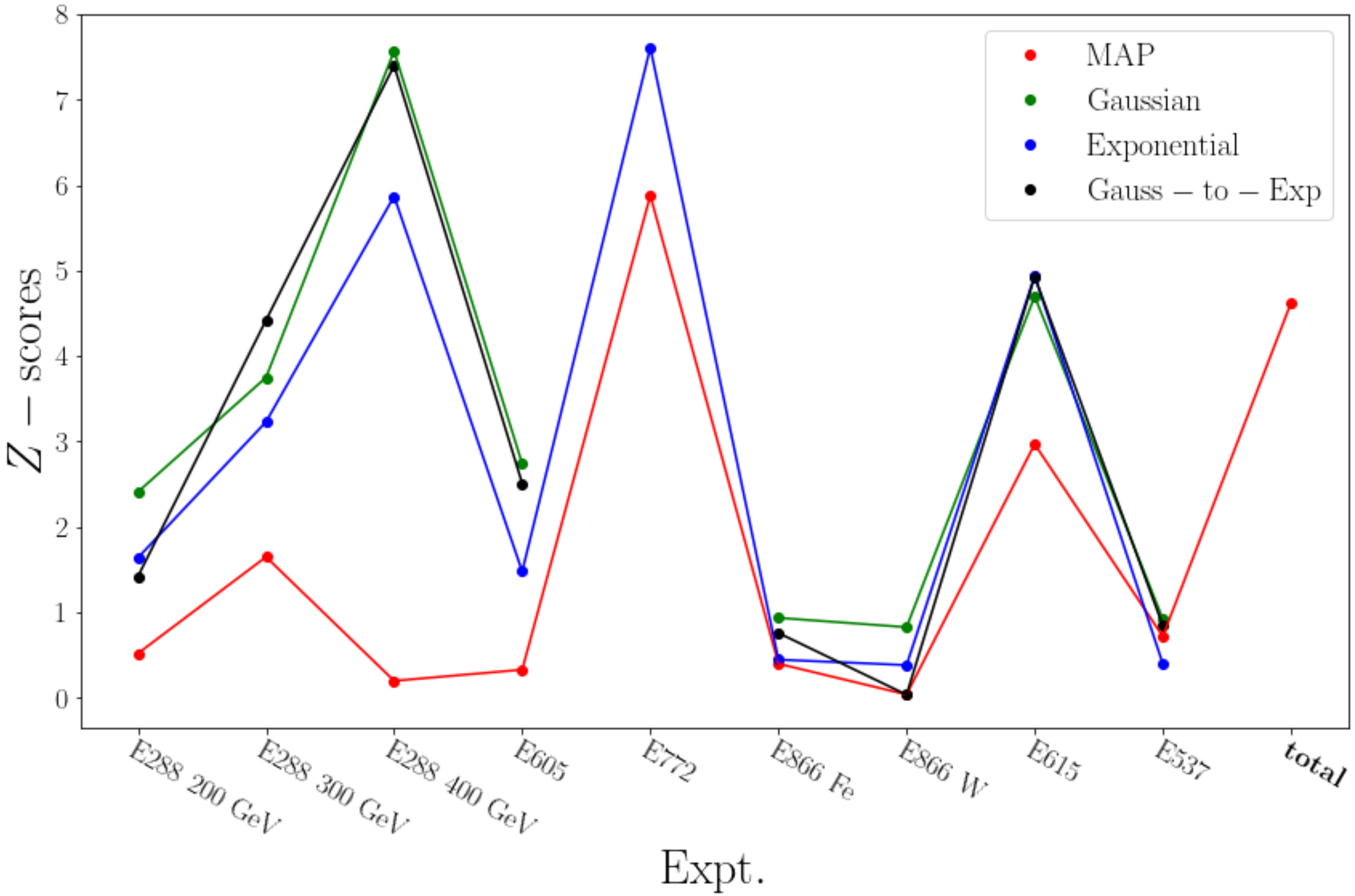

Perturbative orders

- Perform single fit to determine the effects on the non-perturbative objects
- Red and blue curves correspond to previous page
- Conclusion: no difference for these fixed-target kinematics

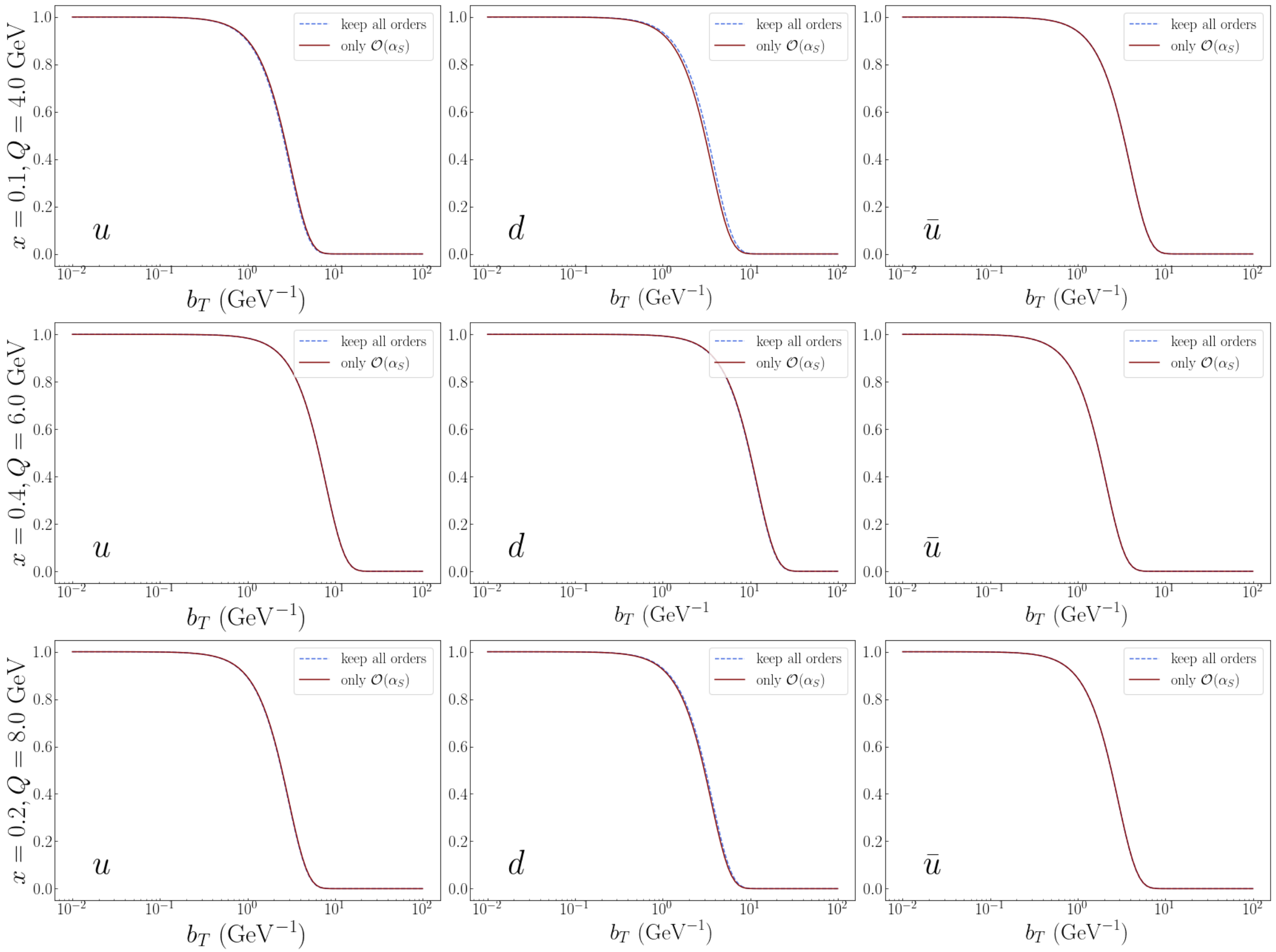

A brief word on $b_{\max}$

- The $b_{\max}$ parameter is a general shift from perturbative to non-perturbative description in $\widetilde{W}$
- Left: $b_{\max} = 2e^{-\gamma_E}/m_c$ Right: $b_{\max} = 0.5\ \mathrm{GeV}^{-1}$

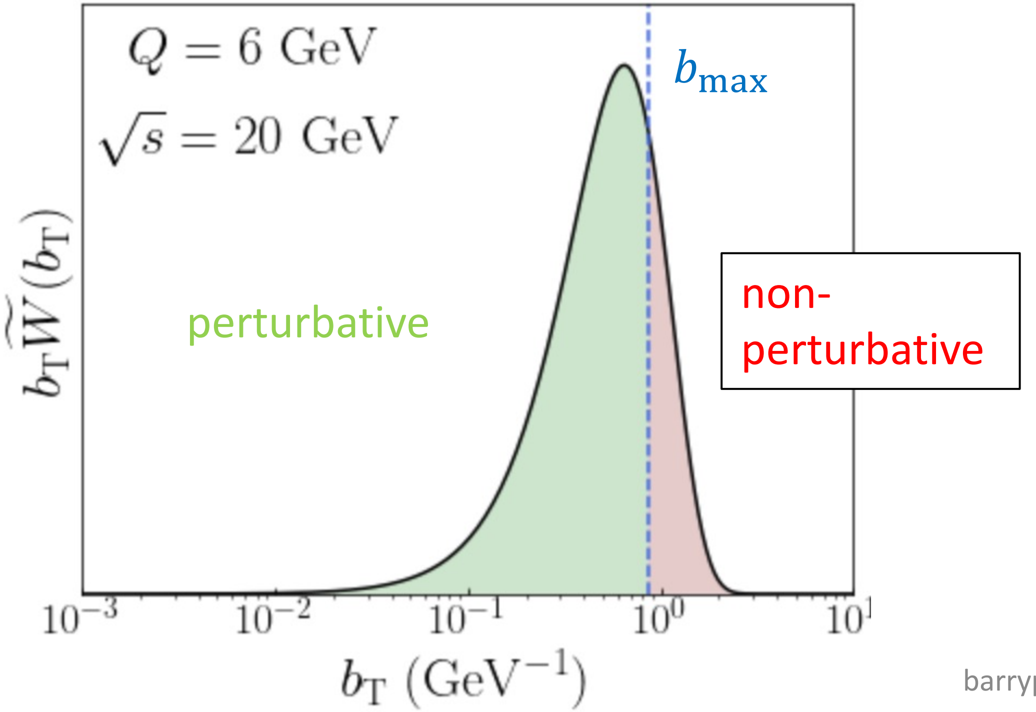

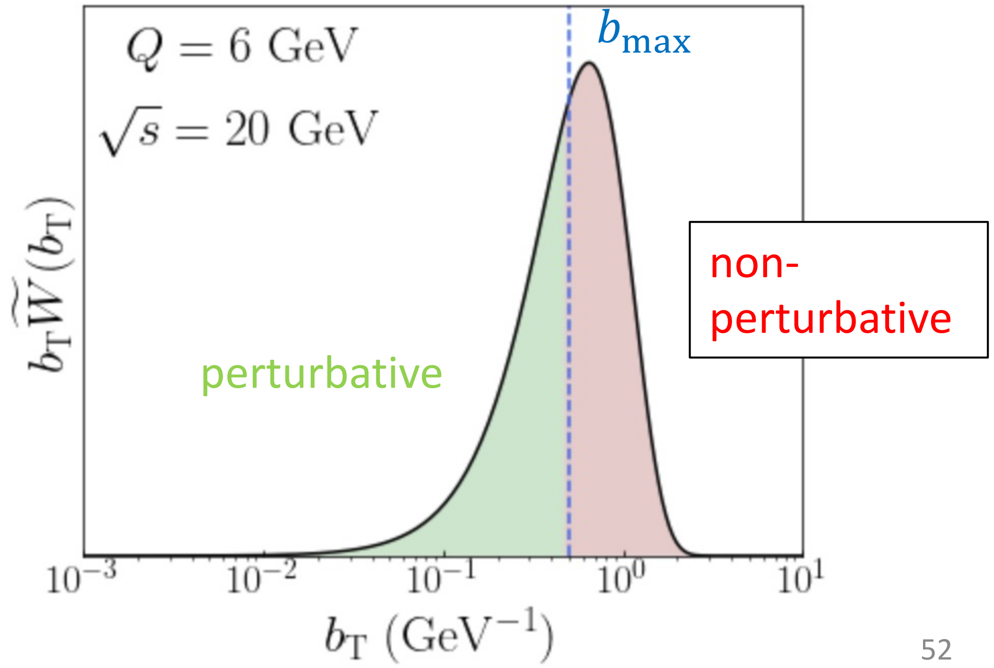

Result from changing $b_{\max}$

- While the agreement with the data is roughly the same, the biggest effect is in the normalizations
- Fitted normalization parameters show a needed enhancement on the resulting theory when decreasing the $b_{\max}$

Extensions

- While fixed-target DY may not greatly probe the collinear PDFs, collider data at e.g. the LHC may have greater constraints